Journal of Science & Technology in the Tropics

Volume 3 Number 1 June 2007

JOSTT

DEDICATED TO THE ADVANCEMENT OF SCIENCE AND TECHNOLOGY RELATED TO THE TROPICS

Journal of Science & Technology in the Tropics

AKADEMI SAINS MALAYSIA

COSTAM

Volume 3 Number 1
June 2007
ISSN 1823-5034

Journal of Science & Technology in the Tropics Volume 3 Number 1 June 2007

CONTENTS

Editorial
Augustine S. H. Ong 3

Quality assurance: Towards diagnostic parasitology practices par excellence
Praphathip Eamsobhana 5

Plasma technology research and development at University of Malaya
C. S. Wong 11

Surface modification of rayon fiber using pulsed plasma generated from theta pinch device
S. Chuenchon, P. Kamsing, R. Mongkolnavin, V. Pimpan and C. S. Wong 21

Low-cost hydrocarbon templated sol-gel synthesis of functional nanoporous silica xerogel
M. Halina, Y. M. Ambar and S. Ramesh 27

Extraction of *Elaeis oleifera* mesocarp and kernel oils using supercritical carbon dioxide
Harrison Lik Nang Lau, Yuen May Choo, Ah Ngan Ma and Cheng Hock Chuah 33

2-Fluoropyrimidine: A potential fluorogenic reagent
Z. Abdullah, M. A. A. Bakar, Z. Aiyub and R. Yahya 39

Changes in physicochemical characteristics of oil palm frond after NaOH treatment towards improved heavy metal sorption
A. Z. Abdullah, B. Salamatinia, N. Razali and A. H. Kamaruddin 45

Development of seismic hazard maps for Peninsular Malaysia
Azlan Adnan, Hendriyawan, Aminaton Marto and Masyhur Irsyam 51

Reviews 59

Journal of Science and Technology in the Tropics (2007) **3:** 11-19

Plasma technology research and development at University of Malaya

C. S. Wong
Plasma Research Laboratory, Physics Department, University of Malaya,
50603 Kuala Lumpur, Malaysia
(Email: cswong@um.edu.my)

Received 06.04.2007; accepted 25.04.2007

Abstract The Plasma Technology Research Group at the Physics Department, Faculty of Science, University of Malaya has developed several areas of plasma technology including pulsed plasma radiations sources, glow discharge type plasmas for material processing and dielectric barrier atmospheric discharges. Some possible future directions are (a) to utilise the plasma focus as a beam target neutron source for neutron activation applications; (b) to use the high energy pulsed ion beam from the plasma focus for applications in nano scale surface modification and in the crystallization of amorphous hydrogenated carbon thin film; (c) to establish the vacuum spark and the capillary discharge as pulsed EUV point sources at 13.5 nm wavelength and to set up a nanolithography system based on these sources; (d) to set up a glow discharge dusty plasma system for the studies of the micro cluster formation and the simulation of astronomical phenomena inside such a plasma; (e) to construct a prototype ozonizer plant with output capacity of 10 grams per hour based on the dielectric barrier discharge for application in water treatment; (f) to test the dielectric barrier discharge for various chemical syntheses such as the decomposition of NO_x and SO_x gases; and (g) to set up a pen-like glow discharge torch based on the dielectric barrier discharge for surface disinfection applications.

Keywords plasma technology – radiation sources – neutron activation – nanolithography – material processing – chemical syntheses

INTRODUCTION

Plasma technology is often referred to as one of the critical technology of the 21st Century. In the developed countries such as the United States of America and Japan, intensive scientific efforts and large funding are being directed at research to develop plasma technologies that are useful for industry. In recent years, newly developed countries such as South Korea and China (including Taiwan) have also joined the race in the quest to be at the frontiers in this area of technology development. The effects of such efforts on the national economy of these countries are obvious.

In view of the importance of plasma technology, we believe that it is necessary for Malaysia to embark on a programme to establish a scientific base for plasma technology so that we will not just play a user role but also to be a contributor to this technology. Plasma technology is indeed a multidisciplinary technology. It is an integration of knowledge and expertise in various disciplines of science and engineering. The expertise and human capital in plasma technology will also be able to complement other important areas of technology such as nanotechnology, microelectronics, photonics and optoelectronics, environmental management and even biotechnology.

It was with great foresight that the Plasma Research Laboratory was established at the Physics Department, Faculty of Science, University of Malaya in the 1960s by the then Head of Physics Department, Prof Dr Thong Saw Park. Early work was focused on the studies of oscillation in the glow discharge and electromagnetic shock waves. In the late 1960s to early 1970s, work on pulsed

power was started with the setting up of a 40 kV 60 μF capacitor bank, which was used to power the first plasma fusion device in South East Asia – the plasma focus.

From 1992, the scope of expertise development by the group was widened and enhanced to cover other types of plasma technology. As of today, the various areas of plasma technology that have been established by the group include:

(a) Pulsed plasma radiation sources including the plasma focus, the vacuum spark and the pulsed capillary discharge. These devices are rich sources of neutron (plasma focus), X-ray, electron and ion beams, and extreme ultraviolet (EUV) radiation.
(b) Glow discharge type plasmas (RF, DC and AC powered) for material processing. Processes tested include nitriding, sputter-coating of titanium nitride, diamond film coating, polymerization.
(c) Dielectric barrier atmospheric discharge as ozonizer and as reactor for decomposition of toxic gases/pollutants.
(d) Other associated technologies such as high power pulsed technology and pulsed radiation detection techniques.

AREAS OF EXPERTISE DEVELOPED

Over the years the effort of the group has been focused on a few areas of plasma technology which can be broadly categorized into three main areas: pulsed, high temperature and high density plasmas; low temperature, low density discharge type plasmas; and atmospheric plasmas.

Pulsed, high temperature and high density plasmas

The plasma focus. The fundamental supporting technology for this type of plasmas is pulsed power engineering. The 40 kV, 2 MA capacitor bank [1] built in the 1970s was the first ever designed and built in Malaysia. It was a landmark achievement at that time and it was used to power the first plasma fusion device, the plasma focus, in the South East Asia region. Deuterium fusion neutrons were detected and reported in 1975 [2] and it marked an important milestone of the plasma technology development in Malaysia. Since then, the plasma focus remains one of the main areas of research in this laboratory until today [3,4].

The plasma focus was proposed in the 1960s as a possible device to achieve thermonuclear fusion. In 1962, a research team at the Kurchatov Institute in USSR (Russia) led by Filippov proposed a modification to the linear Z-pinch by providing an inversed pinch phase as a pre-pinch phase [5]. This pre-pinch phase provides some preliminary heating of the plasma before the radial pinching action starts. A similar concept was proposed by Mather and his team in 1964 at the Los Alamos National Laboratory in USA [6]. The Mather design of the plasma focus was originated from the electromagnetic shock tube and in addition to the inverse pinch phase, a second phase of axial acceleration was added as the pre-pinch heating mechanism.

An obvious difference in the two designs is in their geometrical appearences. The Filippov design has a short and large diameter inner electrode while the Mather design has a long and small diameter inner electrode. The Mather type design has the advantage that a discharge with relatively slow rise-time can be used. The pinch is arranged to occur at the time when the discharge current has reached its maximum. This results in an efficient pinch and a fusioning plasma can be obtained with nominal input electrical energy of a few kJ. It is probably for this reason that the Mather type plasma focus is curently more widely studied, even at small laboratories with low annual budget. Recently, a Mather type plasma focus device with only several tens of joules of input energy has been demonstrated [7]. The current trend in plasma focus research is in its applications as a pulsed neutron, radiation (EUV to X-ray) and charged particle (electron and ion) beams source for industrial applications.

The plasma focus discharge dynamics can be described as consisting of three main phases: (1) the inverse pinch (or lift-off) phase, (2) the axial acceleration phase, and (3) the radial compression (pinch) phase. In the Filippov type plasma focus, the axial phase is practically non existent; while in the Mather type, this phase plays a major role in the focus dynamics. The main plasma heating occurs during the radial compression phase. The plasma formed at the end of this phase has electron temperature of several keV and electron density of up to 10^{19} cm^{-3}. With such a high temperature and

density, the focused plasma is a rich source of X-ray, electron and ion beam and when deuterium is used as the working gas, fusion neutrons will be produced.

The first plasma focus system set up in this laboratory was the UMDPF1, which was optimized to produce fusion neutron yield of 10^9 neutrons per discharge [8]. Several studies were also conducted to characterize the discharge dynamics [9] and X-ray emission of the plasma produced [10].

In 1985, the Plasma Research Group at the University of Malaya was commisioned by the United Nations University (UNU) to conduct a training programme to train eight UNU Fellows from six developing countries including Egypt, India, Indonesia, Nigeria, Pakistan and Sierra Leone. For the purpose of the training programme and the subsequent technology transfer, a small plasma focus powered by a single capacitor rated at 15 kV, 30 μF was designed and successfully tested. This is the UNU/ICTP PFF (United Nations University/ International Centre of Theoretical Physics Plasma Fusion Facility) [11]. The UNU/ICTP PFF (Fig. 1) is currently being used as a source of neutrons, X-rays, ion and electron beams for various applications by various research groups in Pakistan, India, Thailand as well as Singapore besides Malaysia. The device is able to consistently produce neutron yield of up to 10^8 neutrons per discharge. However, our studies show that these neutrons are produced by two mechanisms, the thermonuclear as well as the beam target [4]. The beam target component is produced by the bombardment of the ambient deuterium gas by the high energy deuteron beams. The energies of these deuteron beams have been determined by the time of flight techniques to be greater than 100 keV [3].

Besides the conventional mode of operation as described above, various alternative modes of operation of the plasma focus have also been tested in this laboratory. A possible application of the plasma focus considered by our group is to use it for nano-scaled modification of materials such as to change amorphous silicon to single crystal silicon. For this purpose, the operation of the plasma focus in three modes have been proposed: (a) the normal focusing mode where the combination of a high energy ion beam and a hot dense plasma jet [12] can be obtained; (b) the low pressure mode where the focussing action is obstructed so that only the high energy ion beam will be produced [13], without the subsequent plasma jet; and (c) the electromagnetic shock tube mode of operation to generate only the hot dense plasma jet [14], without the ion beam. A proposal to study the possible effect of the high energy ion beam, or the hot dense plasma jet, or the combined effect of the two on nano-scaled modification of material has recently received funding from the Science Fund awarded by the Ministry of Science, Technology and Innovation (MOSTI).

A bench-top plasma focus powered by ten door knob ceramic capacitors each rated at 40 kV, 2.7 nF has been designed and constructed recently and is

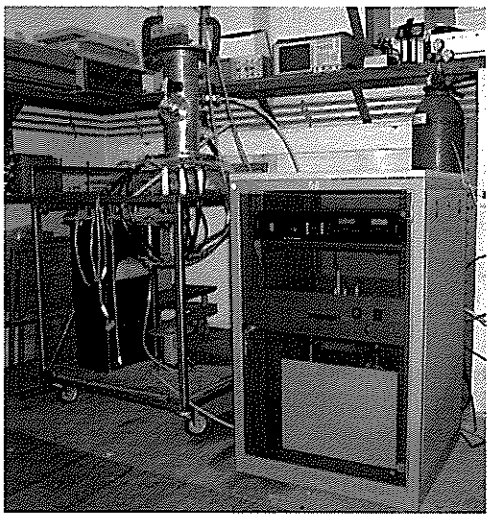

Figure 1. The UNU/ICTP PFF plasma focus system.

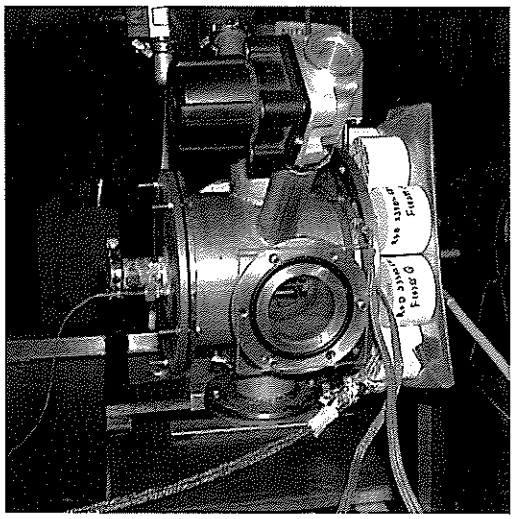

Figure 2. The bench-top plasma focus system.

now being tested for production of focussed plasma (Fig. 2). This device, the University of Malaya Campact Plasma Focus (UMCPF), with scaled down input electrical energy of 22 J is expected to produce a focused plasma with a volume much smaller than that produced by the UNU/ICTP PFF but with similar plasma condition of electron temperature T_e ~ several keV and electron density n_e ~ 10^{18} cm^{-3}. With deuterium as the working gas, it may be operated as a repetitive beam target neutron source for neutron activation applications.

The vacuum spark and related devices. Another type of devices that has been developed is the vacuum spark and its varied modes of operation. Traditionally, the vacuum spark is being used as an intense X-ray source capable of emitting line radiations that correspond to highly ionized state of metallic plasma produced by passing a high current (~100 kA) through the metallic vapour of the anode material. Due to the resemblance of its X-ray emission spectrum to that of the solar flare phenomenon, it is often used to simulate such phenomenon in the laboratory and to calibrate detection system to be used to study the phenomenon.

In this laboratory, the successful operation of a laser initiated vacuum spark system was first reported in 1984 [16]. Since then, various innovative developments in the technology of the device have been carried out. The operation of the device has been optimized to reduce the size of the capacitor bank to merely one-twelth (1/12) of the system reported in 1984 [16], and the laser triggering has been replaced by transient hollow cathode discharge (THCD) electron beam triggering [17].

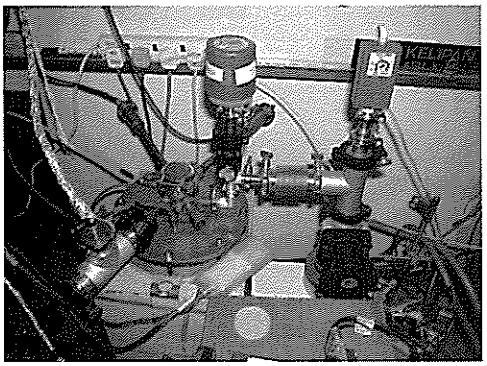

Figure 3. The vacuum spark device.

This resulted in a mobile vacuum spark system powered by a single capacitor rated at 40 kV, 1.85 μF, which is more convenient for application. This system (Fig. 3) is now a well characterized pulsed, intense, point X-ray source ready to be used for radiography of nano-scaled substances, including biological and metallic samples. Further development on this device is to scale its input energy downwards to produce a plasma appropriate for emission in the EUV region. Specifically, the wavelength required by the industry for the next generation lithography for the printing of submicron pattern is 13.5 nm. For the purpose of generating emission at this wavelength, copper and tin plasmas are being tested [18]. A 20 kV, 22 nF vacuum spark discharge operated in a repetitive mode is believed to be a suitable source for this purpose.

The pulsed discharge technology developed using the vacuum spark has also been diversified further and leading to the design of three devices: the flash X-ray tube, the pulsed capillary discharge and the exploding wire. In the flash X-ray tube

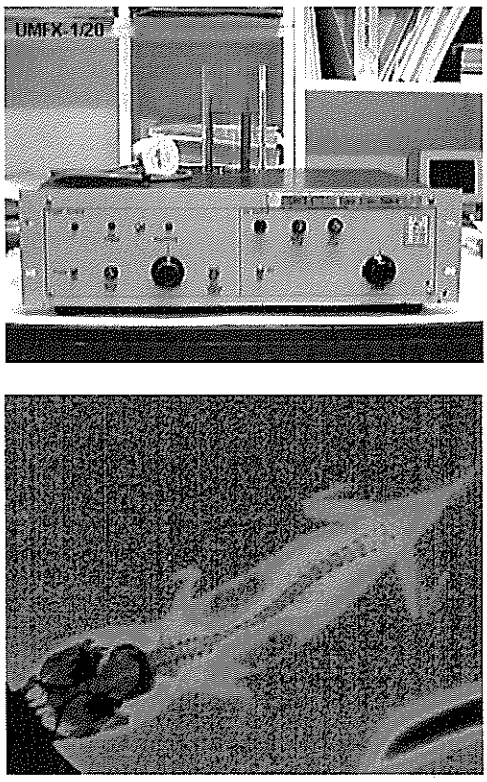

Figure 4. The UMFX flash x-ray source and an example of radiogaph of a live lizard taken using the source.

[19, 20], the capacitor bank is scaled down to 20 kV, 3.3 nF with an input electrical energy of only 0.66 J. The temperature of the plasma produced by this discharge will be too low to generate X-ray. However, a sufficiently intense pre-discharge X-ray pulse consisting of characteristic line radiation of the anode material produced by the bombardment of THCD electron beam at the anode will be obtained. The device is a bench top wavelength tunable pulsed X-ray source that may be used for radiography of small sample including biological sample such as the lizard (Fig. 4).

When the small vacuum space (with a typical gap of <5 mm) between the electrodes of the vacuum spark is filled by a block of insulator (for example teflon) with a quartz or alumina capillary with diameter of 1 to 3 mm and length of 5 mm or less along its axis, the device is now being operated as a pulsed capillary discharge (Fig. 5) [21]. When viewed from the end-on direction, a circular source with a hot dense core of plasma is produced, emitting intensely in the EUV region. The aim is to produce a plasma (argon or xenon) with electron temperature of about 10 to 50 eV. Such a plasma consists of ionic species which emit line radiation with wavelength of around 13.5 nm. A key experiment to determine the time resolved imaging of the source structure and the time resolved EUV spectrum emitted by the plasma is now being carried out with support of a grant awarded by the Ministry of Higher Education (MOHE) under the Fundamental Research Grant Scheme (FRGS).

Another variation of the vacuum spark system is obtained by connecting a thin wire across the electrodes. When the discharge is initiated, high current of tens of kA will flow through the wire, vapourizing it to form a plasma. Such a plasma may consist of nano sized particles of the wire material. This is the exploding wire discharge which is being considered as one of the techniques to synthesize nano particles. Work on this technique has just been started using the support of a Scientific Advancement Grant Allocation (SAGA) awarded by the Academy of Sciences Malaysia (ASM).

Low temperature, low density glow discharge type plasmas

These are sometimes referred to as industrial plasmas as they are currently widely used in many areas of industry. They are either in the form of corona discharge, glow discharge, or arc discharge. In contrast to the high temperature and high density plasmas which must be produced by pulsed discharge, low temperature and low density plasmas can be produced by using either DC or AC power source. AC power source of various frequencies can be used but the frequency commonly used by the industry is the 13.56 MHz radio frequency (RF). Low temperature, low density plasmas can also be heated by using microwave power source, in which the heating mechanism is via wave phenomena.

Presently, our effort in the development of low temperature and low density plasma is focused on direct electrical heating using either DC or AC (13.56 MHz, and various other non-conventional frequencies) power source. For the experiment using the 13.56 MHz power source (Fig. 6), we have adopted the planar coil inductively coupled

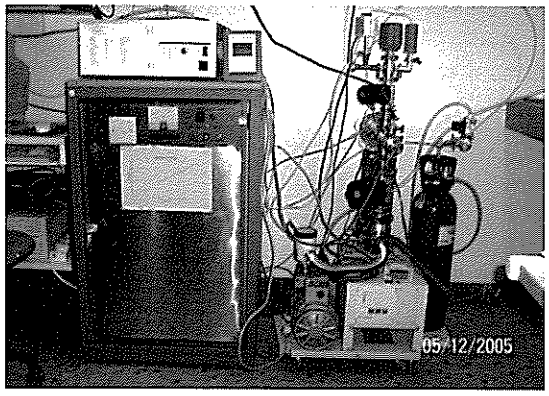

Figure 5. The pulsed capillary discharge EUV source.

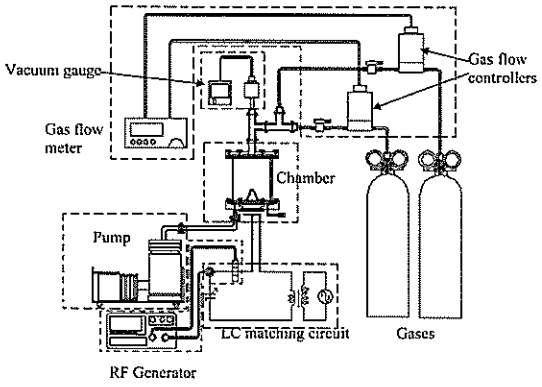

Figure 6. RF planar inductively coupled plasma system.

configuration. This configuration has the advantage of being able to produce a disc-like plasma with large cross sectional area. This means sample with larger area can be processed. For the matching network, we use an innovative LC resonant circuit concept [22] instead of the conventional π network that is available commercially. This not only helps to reduce the cost of the work, operating at resonant condition will also mean more efficient energy transfer.

An interesting feature of the RF Planar Coil Inductively Coupled Plasma (RF PCICP) is the observation of two modes of operation, the E-mode and the H-mode operation [23]. In the E-mode operation, the plasma is heated by current driven in the radial direction. This mode is dominant at low RF power. When the RF power is increased to a sufficiently high level, electrical breakdown in the azimuthal (in the θ-direction with reference to a cylindrical coordinate) direction will occur. Once this happens, the discharge is in the H-mode operation and the electron density may be increased by two order of magnitude, although the electron temperature may still remain about the same as in the E-mode operation. The increase in the electron density is probably due to the toroidal current path which results in higher cross-section for ionizing collision by the electrons. Such an abrupt increase in the electron density can be visually detected. When H-mode discharge is obtained, a bright hemispherical plasma can be observed to be attached to the quartz window of the plasma chamber (Fig. 7).

The RF PCICP has been tested for various material processing applications such as nitriding of stainless steel [24], nitriding of titanium [25], sputter coating of titanium nitride onto stainless steel surface [26], and coating of diamond like carbon (DLC) film. Recently, the formation of carbon nano tubes [27] in this type of plasma has also been investigated.

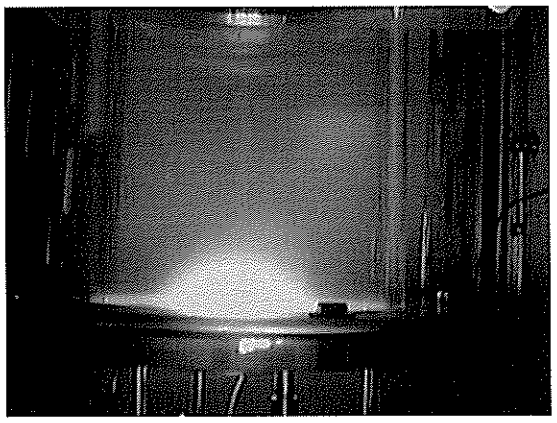

Figure 7. H-mode discharge of the RFICP.

Another interesting area of research related to the glow discharge type of plasma is the study of stochastic behaviour of micron to nano size particles in a plasma environment, the so called dusty plasma or complex plasma [28]. The studies on the nonlinear oscillation of these particles and the nature of binding forces between them leading to crystal formation in such a plasma are significant in the understanding of astronomical phenomena as well as in plasma processing of materials. A project to set up and study the dusty plasma has been initiated with the submission of a Science Fund application to the Ministry of Science, Technology and Innovation (MOSTI).

Atmospheric plasmas

Dielectric barrier discharge. The dielectric barrier discharge (DBD) is a special type of atmospheric discharge where the electrodes are physically blocked by a dielectric so that electrical breakdown cannot occur even with high electric field applied across the electrodes. Intermittent sparks occur in the space between the dielectric surface and one of the electrodes when the charge accumulation caused by polarization effect reaches a high enough density. An alternating high voltage is required to induce the occurrence of the intermittent spark, and the probability of occurrence increases with the frequency as well as the magnitude of the alternating voltage. When a gas is flown through the space where the intermittent sparks occur, chemical reaction of the gas can be induced. An example is the conversion of oxygen into ozone. Such a discharge is used to produce the plasma ozonizer developed in this laboratory. Other types of chemical reactions are also possible, for example the breaking down of NO_X and SO_X contained in the exhaust gas of a power generating station, or the car engine.

Ozonizers based on the dielectric barrier discharge have been developed under the 8th Malaysia Plan. A two tubes bench top unit (Fig. 8) capable of producing 0.7 gram of ozone per hour

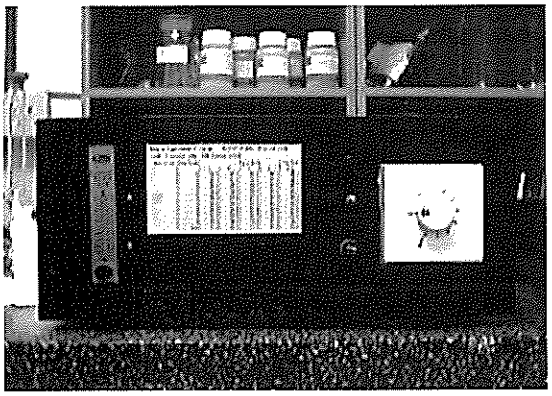

Figure 8. Two tubes bench top ozonizer unit.

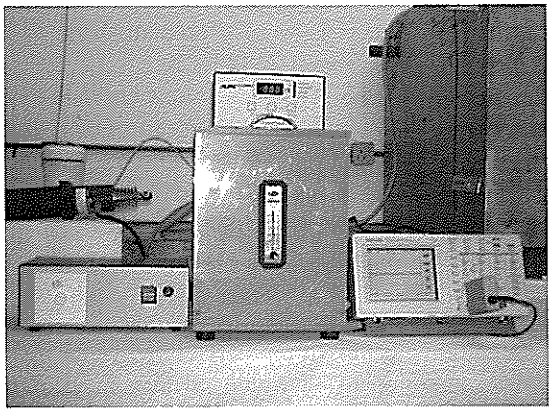

Figure 9. Ten tubes plasma ozonizer module.

is useful as a laboratory unit for testing various ozonation processes. For example, the plasma ozonizer had been used to show in the laboratory the effectiveness of using ozonation to treat textile waste effluent [29]. The ten tubes unit (Fig. 9) is built as a module of ozonizer plant for industrial application such as treatment of swimming pool water. This module is capable of producing 5.4 grams of ozone per hour. Higher ozone output can be obtained by stacking up multiple units of this module.

Besides the development of ozonizers based on the DBD, a project to test the decomposition of NO and NO_2 using the DBD reactor is now on-going. It is believed that the DBD developed in this laboratory can be established as a plasma reactor for various chemical syntheses, thus opening up tremendous prospects for applications.

Atmospheric glow discharge. High power atmospheric arc discharge has long been used to produce thermal plasma as a heat source capable of generating gas temperature as high as 20,000 K. Such a heat source is at the heart of the plasma gasification and vitrification system used for the complete decomposition of solid wastes [30]. On the other hand, the atmospheric glow discharge has recently received much attention [31,32] due to the realization of its potential in the field of food preservation and in medicine. A small pen-like atmospheric glow discharge (plasma pen) [33] has been demonstrated to be able to disinfect wound and other small surfaces. This will provide opportunity for plasma technology to be linked to biological science. This will be established as one of the directions of our group's work in the area of low temperature plasmas. A proposal to develop atmospheric glow discharge and its application to biological systems has been approved under the Science Fund.

CONCLUSION

Dedicated research carried out at the Plasma Research Laboratory, Physics Department, University of Malaya during the last 40 years has been consolidated and strengthened by the current team of researchers. It is the effort of three generations of researchers that takes the laboratory to the present height. With the achievements recorded so far, there is no doubt that the laboratory can be considered a world class laboratory and the group is playing a leadership role in helping developing countries to initiate and strengthen research in plasma technology [34]. It is important that the group's research effort continues to receive support at the university level as well as at the national level.

Acknowledgements – The establishment and development of the University of Malaya Plasma Research Laboratory would not have been possible without the financial support given by the Government of Malaysia through the Ministry of Higher Education and the Ministry of Science, Technology and Innovation. Many people have contributed significantly to the achievements of the laboratory, which include S.P. Thong, H.H. Teh, B.C. Tan, S. Lee, Y.H. Chen, A.C. Chew, S.P. Moo and many others. The technical and administrative supports given by the technical assistants and laboratory assistants, in particular W.T. Loo, Jasbir Singh and Seniah Ariffin who are currently still in

service, are very much appreciated. Last but not least, all the graduate students (too numerous to be mentioned here) who have been involved in the projects carried out in the laboratory since the 1960s are also gratefully acknowledged.

REFERENCES

1. Thong S.P. and Lee S. (1973) A simplified method of switching a 2 mega-ampere capacitor bank using a voltage division technique. *Mal. J. Sci.* **2A:** 157-169.
2. Lee S. and Chen Y.H. (1975) Measurement of neutrons from a focused plasma. *Mal. J. Sci.* **3B:** 159-163.
3. Wong C.S. and Yap S.L. (2005) Generation of deuteron beam from the plasma focus. *Solid State Phenomena* **107:** 151-155.
4. Yap S.L., Wong C.S., Choi P., Dumitrescu C. and Moo S.P. (2005) Observation of two phases of neutron emission in a low energy plasma focus. *Jpn. J. Appl. Phys.* **44:** 8125-8132.
5. Filipov N.V., Filipova T.I. and Vinogradov V.P. (1962) Dense, High-Temperature Plasma in a Noncylindrical 2-pinch Compression. *Nucl. Fusion* **2** (Suppl.): 577.
6. Mather J.W. (1964) Investigation of the High-Energy Acceleration Mode in the Coaxial Gun. *Phys. Fluids* **7:** S28-34.
7. Silva P., Soto L., Kies W. and Moreno J. (2004) Pinch evidence in a fast and small plasma focus of only tens of joules. *Plasma Sources Sci. Technol.* **13:** 329-332.
8. Chen Y.H. (1978) *Parametric studies of focus optimization.* PhD thesis, University of Malaya.
9. Chow S.P., Lee S. and Tan B.C. (1972) Current sheath studies in a co-axial plasma focus gun. *J. Plasma Phys.* **8:** 21-31.
10. Wong C.S., Moo S.P., J. Singh, Choi P., Dumitrescu-Zoita C. and Silawatshananai C. (1996) Dynamics of x-ray emission from a small plasma focus. *Mal. J. Sci.* **17B:** 109-117.
11. Lee S., Tou T.Y., Moo S.P. et al. (1988) A simple facility for the teaching of plasma dynamics and plasma nuclear fusion. *Am. J. Phys.* **56:** 62-68.
12. Lee S., Harith A., Tou T.Y., et al. (1985) Dynamics of REB-sputtered coper plasma jet. *J. Fiz. Mal.* **6:** 23-28.
13. Wong C.S., Choi P., Leong W.S. and Jasbir S. (2002) Generation of high energy ion beams from a plasma focus modified for low pressure operation. *Jpn. J. Appl. Phys.* **41:** 3943-3946.
14. Lee S., Eissa M., Gholap A.V., et al. (1986) Toroidal plasmoids in an electromagnetic shock tube. *Singapore J. Phys.* **3:** 75-82.
15. Lee T.N. (1974) Solar flare and laboratory plasma phenomena. *The Astrophysical J.* **190:** 467-479.
16. Wong C.S. and Lee S. (1984) Vacuum spark as a reproducible x-ray source. *Rev.Sci.Instrum.* **55:** 1125-1128.
17. Wong C.S., Ong C.X., Moo S.P. and Choi P. (1995) Characteristics of a vacuum spark triggered by the transient hollow cathode discharge electron beam. *IEEE Tran. Plasma Sci.* **23:** 265-269.
18. Chew S.H. and Wong C.S. (2006) X-ray and euv emission characteristics of a vacuum spark. *J. Sci. Technol. in the Tropics* **2:** 125-129.
19. Wong C.S., Lee S., Ong C.X. and Chin O.H. (1989) A compact low voltage flash X-ray tube. *Jpn. J. Appl. Phys.* **28:** 1264-1267.
20. Bradley D.A., Wong C.S. and Ng K.H. (2000) Evaluating the quality of images produced by soft x-ray units. *Applied Radiation and Isotopes* **53:** 691-697.
21. Yap L.M., Zanuldin A. and Wong C.S. (2005) Operation of a pulsed capillary discharge for in-band EUV emission to be employed in next generation lithography. *J. Fiz. Mal.* **26:** 45-49.
22. Ng K.H., Liew W.S., Roslan M.N. and Wong C.S. (2002) A planar coil inductively coupled plasma system for thin film deposition. *J. Fiz. Mal.* **23:** 51-53.
23. Kok Y.C. and Wong C.S. (1998) A low power planar coil inductively coupled plasma system. *J. Fiz. Mal.* **19:** 31-36.
24. Chakrabarty C.K., Azmi I., Wong C.S. and Kok Y.C. (1998) Inductively coupled RF plasma nitriding of steels. *Processing and Fabrication of Advanced Materials VI,* ed. K.A. Khor, T.S. Srivatsan and J.J. Moore: 1197-1207.
25. Abdul H.H. and Wong C.S. (2002) Nitriding of titanium by spiral coil radio frequency inductively coupled plasma. *J. Fiz. Mal.* **23:** 39-42.
26. Chew S.P. and Wong C.S. (2002) Coating of titanium nitride thin film on stainless steel using an rf planar coil inductively coupled plasma. *Mal. J. Sci.* **21:** 107-113.
27. Lee C.C., Tamil M.T., Roslan M.N., Chin O.H. and Wong C.S. (2005) Parametric effect of carbon nanotubes synthesis using a CVD technique. *Paper presented at International Meeting on Frontiers of Physics(IMFP 2005), 25-29th July 2005, Kuala Lumpur.*
28. Ticos C.M. and Smith P.W. (2006) Dusty plasma and

a review of the research a Oxford. *J. Fiz. Mal.* **27:** 1-7.
29. Rajeswari K.R., Noorsaadah A. R. and Wong C.S. (2001) Effect of temperature on the ozonation of textile waste effluent. *Color Technol.* **117:** 95-97.
30. Kogelschatz U. (2004) Atmospheric-pressure plasma technology. *Plasma Phys. Control. Fusion* **46:** B63-75.
31. Montie T.C., Wintenberg K.K. and Roth J.R. (2000) An overview of research using the one stmosphere uniform glow discharge plasma (OAUGDP) for sterilization of surfaces and materials *IEEE Trans. Plasma Sci.* **28:** 41-50.
32. Wang X.X., Li C.R., Lu M.Z. and Pu Y.K. (2003) Study on an atmospheric pressure glow discharge. *Plasma Sources Sci. Technol.* **12:** 358-361.
33. Janca J., Klima M., Slavicek P. and Zajickova L. (1999) HF plasma pencil – new source for plasma surface processing. *Surface and Coating Technol.* **116-119:** 547-551.
34. Lee S. and Wong C.S. (2006) Initiating and strengthening plasma research in developing countries. *Physics Today* **59:** 31-36.

JOURNAL OF SCIENCE AND TECHNOLOGY IN THE TROPICS

NOTICE TO CONTRIBUTORS

JOSTT is a multi-disciplinary journal. It publishes original research articles and reviews on all aspects of science and technology relating to the tropics. All manuscripts are reviewed by at least two referees, and the editorial decision is based on their evaluations.

Manuscripts are considered on the understanding that their contents have not been previously published, and they are not being considered for publication elsewhere. The authors are presumed to have obtained approval from the responsible authorities, and agreement from all parties involved, for the work to be published.

Submission of a manuscript to JOSTT carries with it the assignment of rights to publish the work. Upon publication, the Publishers (COSTAM and ASM) retain the copyright of the paper.

Manuscript preparation

Manuscripts must be in English, normally not exceeding 3500 words. Type double spaced, using MS Word, on one side only of A4 size with at least 2.5 cm margins all round. Number the pages consecutively and arrange the items in the following order: title page, abstract, key words, text, acknowledgements, references, tables, figure legends.

Title page

Include (i) title, (ii) names, affiliations and addresses of all authors, (iii) running title not exceeding five words, and (iv) email of corresponding author.

Abstract and key words

The abstract, not more than 250 words, should be concise and informative of the contents and conclusions of the work. A list of not more than five key words must immediately follow the abstract.

Text

Original research articles should be organized as follows: Introduction, Materials and Methods, Results, Discussion, Acknowledgement, References. The International System of Units (SI) should be used. Scientific names and mathematical parameters should be in italics.

References

References should be cited in the text as numbers enclosed with square [ ] brackets. The use of names in the text is discouraged. In the reference section, the following examples should be followed:

1 Yong H.S., Dhaliwal S.S. and Teh K.L. (1989) A female Norway rat, *Rattus norvegicus*, with XO sex chromosome constitution. *Naturwissenschaften* **76:** 387-388.

2 Beveridge W.I.B. (1961) *The Art of Scientific Investigation*. Mercury Book, London.

3 Berryman A.A. (1987) The theory and classification of outbreaks. *In* Barbosa P. and Schultz J.C. (eds.) *Insect outbreaks* pp. 3-30. Academic Press, San Diego.

Tables

Tables should be typed on separate sheets with short, informative captions, double spacing, numbered consecutively with Arabic numerals, and do not contain any vertical lines. A table should be set up to fit into the text area of at most the entire page of the Journal.

Illustrations

Black-and-white figures (line drawings, graphs and photographs) must be suitable for high-quality reproduction. They must be no bigger than the printed page, kept to a minimum, and numbered consecutively with Arabic numerals. Legends to figures must be typed on a separate sheet. Colour illustrations can only be included at the author's expense.

Proofs and reprints

Authors will receive proofs of their papers before publication. Ten reprints of each paper will be provided free of charge.

Submission

Manuscripts should be submitted in triplicate (including all figures but not original artwork), together with a floppy diskette version of the text, to:

The Managing Editor
Journal of Science and Technology in the Tropics
C-3A-10, 4th Floor Block C, Lift No: 5
No. 1 Jalan SS20/27
47400 Petaling Jaya
Selangor Darul Ehsan
Malaysia

Journal of Science and Technology in the Tropics (2007) **3:** 21-26

Surface modification of rayon fiber using pulsed plasma generated from theta pinch device

S. Chuenchon [1], P. Kamsing[2], R. Mongkolnavin[2], V. Pimpan[1*] and C. S. Wong[3]
[1]Department of Materials Science, Faculty of Science, Chulalongkorn University, 10330 Bangkok, Thailand
[2]Department of Physics, Faculty of Science, Chulalongkorn University, 10330 Bangkok, Thailand
[3]Physics Department, Faculty of Science, University of Malaya, 50603 Kuala Lumpur, Malaysia
(*Corresponding author. E-mail: vimolvan@gmail.com)

Abstract An attempt to test the possibility of using a theta pinch plasma for surface modification of textile fibers was carried out. Rayon fibers were treated by oxygen and nitrogen plasmas produced by a theta-pinch device. With an estimated electron temperature of a few eV, ions with kinetic energy of this order of magnitude could be expected to enter the plasma sheath surrounding the fiber surface. These energetic ions would bombard at the fiber surface and caused the formation of hydrophilic functional groups on the fiber surface as confirmed by FT-IR spectroscopy. When compared to the untreated fiber, all the plasma-treated fibers exhibited a remarkable increase in hydrophilic characteristics such as higher moisture content which caused an increase in diameter and linear density and stronger intermolecular bonds which resulted in higher tenacity. These properties also varied depending on the type of gases and the number of discharges applied.

Keywords plasma – modification – fiber – rayon – theta-pinch

INTRODUCTION

Surface modification of textile fibers has become an alternative way to achieve a textile product having the properties as desired, besides synthesizing a new type of a textile fiber. Conventional modification processes such as graft copolymerization and coating are generally wet processes involving the use of chemicals and solvents. In coating, the fiber surface is coated with an additive or additives to give thin and uniform additive layer in the finishing stage. However, this method often causes problems in fastness. On the other hand, grafting of a polymer onto the fiber surface gives a good fastness but it may affect bulk properties and required much more complicated steps [1]. Recently, many scientific literatures [2-11] have revealed a growing interest in the applications of plasma treatment on textiles due to the numerous advantages over conventional modification processes. For example, in plasma treatment, only the fiber surface is modified without changing any bulk properties. Moreover, it is a dry process which requires much simpler steps and more environmental friendly than the conventional wet processes. Furthermore, this process can be used to modify textile product in many forms including fiber or fabric and almost all compounds including inert gases such as He and Ne and non-polymer forming gases such as NH_3 and CF_4 can be incorporated into a substrate fiber by chemical and physical reactions [1].

Previous works have emphasized on surface modification of both natural and synthetic fibers and fabrics such as poly(ethylene terephthalate), nylon, polyethylene, polypropylene and wool using cold plasmas generated from several devices [2-11]. Because these plasma generating processes are continuous, their electron temperatures are only of the order of 1 eV or less while the ions in the bulk of the plasma are near room temperature (non thermal plasma condition). The ions bombarding at the fiber surface are those entering the plasma sheath surrounding the fiber surface and according to Bohm Criterion, they have kinetic energy of the

same order of magnitude as the electrons in the bulk of the plasma, which is about 1 eV or less. One approach is to apply a negative high potential to the substrate holder (usually metallic) and in order to prevent excessive heating of the fiber this high potential is applied in pulses.

A new approach for surface modification of a textile fiber is by using pulsed plasma, which is the method adopted in the present study. Rayon fiber, a regenerated cellulose fiber, was surface-modified by plasma generated from a low energy theta-pinch device. The dynamic of this device is governed by an increase in magnetic field which induces an electric field opposing to the direction of the discharge current. For a high current operation, the plasma current will interact with its self-magnetic field to produce an electromagnetic force that rapidly compresses toward the tube axis. However, in the present study, the theta pinch is only operated with a primary discharge current of 128 kA. With such a moderate current, we do not expect a strong pinching of the plasma column to occur. However, a plasma with electron temperature of a few eV can be obtained. As a first attempt, this plasma was used to test its effect on rayon fiber surface modification. Discharge parameters including the types of gas and the number of plasma shots were varied. Surface morphology and properties of the treated rayon fiber were investigated and compared to those of the unmodified one.

EXPERIMENTAL SETUP

Materials

The Rayon fiber was provided by Num Rung Rayon Co., Ltd. The fiber was received in the form of yarn. It consists of 24 filaments with the size of 75 deniers and has a melting temperature of 350°F.

Method

A single fiber was removed from rayon yarn. Then it was wound around a brass bar and placed along the axis and in the middle of the theta-pinch device. The theta-pinch device used was donated by the Asian African Association for Plasma Training (AAAPT). In this work, it was operated with a charging voltage of 30 kV and operating pressure of 1 mbar (in oxygen or nitrogen). After the treatment was completed, the fiber was removed from the chamber and analyzed.

Optical microscope (OLYMPLUS BH-2) was used to observe the surface of the fibers. Prior to the test, a sample was placed on the glass slide in horizontal axial. Then it was observed by magnification of 20 times. JSM-6400 scanning electron microscope (SEM) was also used to characterize the sample morphology. Prior to test, a sample was placed on a stub with double sided sticky tape. Then it was coated with thin evaporated layer of gold in order to improve conductivity and prevent electron charging on the surface. The SEM was operated at 15 kV acceleration voltage. SEM photographs were taken at different angles of view with magnification of 2300 times.

The moisture content of the fibers was measured according to ASTM D2654. Each sample was exposed in normal atmosphere at room temperature for 24 hours. After that, the sample was weighed in the condition state and dried at 105 ± 2°C and weighed again to determine the weight change. The moisture content was calculated as the weight difference and reported as percentage of weight decrease from the initial weight using equation 1.

$$\text{Moisture Content, \%} = 100 \times (A-D)/A \quad (1)$$

Where: A = the mass of fiber, mg; and D = the mass of dried fiber, mg.

Fourier transform infrared spectroscopy (FT-IR) was performed using Thermo Nicolet Nexus 670 to characterize the chemical structures of the fibers. A sample was mixed with potassium bromide (KBr) and pressed into the disc form by the hydraulic compression. The samples were scanned at the frequency range of 4000-400 cm^{-1} with 32 consecutive scans and 4 cm^{-1} resolution.

Linear density of the fibers was measured according to ASTM D1577. The untreated and treated fibers were tested in the standard atmosphere for testing of textiles, namely, 21±1°C (70±2°F) and 65±2% relative humidity. Each fiber was cut and its length was measured to the nearest estimated 0.1 mm. Then each fiber was weighed to the nearest 0.0001 mg and its mass was recorded. Linear density of a fiber was calculated using equation 2 with N=1.

$$D = 9000 \times W/(L \times N) \quad (2)$$

Where: D = average fiber linear density, denier; W = mass of bundle specimen, mg; L = length of bundle specimen, mm; and N = number of fibers in the bundle specimen.

Tenacity of the fibers was determined according to ASTM D2256 using Universal testing machine (LLOYD 500). A sample was tested at a testing speed of 300±10 mm/min using a gauge length of 250±3 mm and load cell of 1 N.

RESULTS AND DISCUSSION

The moisture contents measured based on ASTM D2654 of all plasma-treated rayon fibers are higher than that of the untreated one and as the number of plasma shots increases, the moisture content of the fibers increases (Fig. 1). These results suggest the formation of hydrophilic functional groups on the fiber surface and an increase in the number of these groups with increasing number of plasma shots. Furthermore, they also suggest that the functional groups formed on nitrogen plasma-treated fibers are different from those formed on oxygen plasma-treated fibers since the moisture contents of the former are higher than those of the latter.

To confirm these results, the chemical structures of the fibers were determined by Fourier transform infrared spectroscopy (FT-IR) using Thermo Nicolet Nexus 670. Rayon fibers treated with nitrogen plasma exhibit the peak corresponding to C=O bond at 1714 cm^{-1} and narrow peaks at wave number range of 3200-3600 cm^{-1} indicating a decrease in O-H bond and the formation of N-H bond (Fig. 2a). It can be concluded that one type of hydrophilic functional group formed is amide group (HN-C=O). On the other hand, rayon fibers treated with oxygen plasma exhibit broader peaks at wavenumber range of 3200-3600 cm^{-1} and an increase in intensities and splitting of the peaks at wave number of 1600-1650 cm^{-1} (Fig. 2b). This indicates the possibility of the formation of hydroxyl, carboxylic, ketone and aldehyde groups. However, since amide group is more hydrophilic than the other groups, it can absorb higher amount of water. Therefore, the moisture contents of rayon fibers treated with nitrogen plasma are higher than those of rayon fibers treated with oxygen plasma.

The cross-sections of the rayon fibers observed by JSM-6400 scanning electron microscope (SEM) after they were treated with nitrogen and oxygen plasmas are shown in Figure 3. It can be seen that plasma treatment changed the shape of cross-sections of the rayon fibers. They also show the

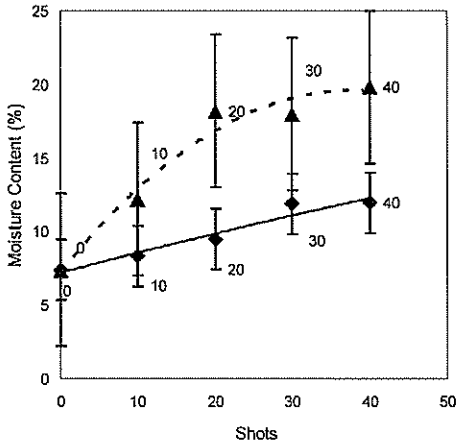

Figure 1. Moisture contents of untreated and plasma-treated rayon fibers. ▲ Rayon (N); ♦ Rayon (O); dash line, Rayon (N); solid line, Rayon (O)

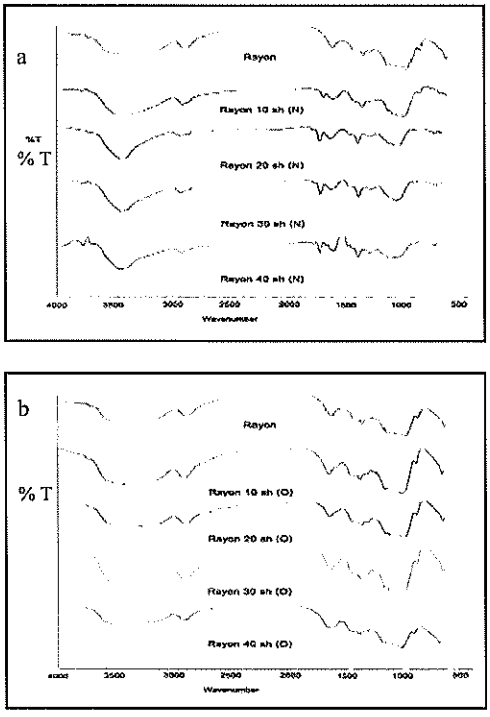

Figure 2. FT-IR spectra of untreated and nitrogen plasma-treated rayon fibers (a), and untreated and oxygen plasma-treated rayon fibers (b).

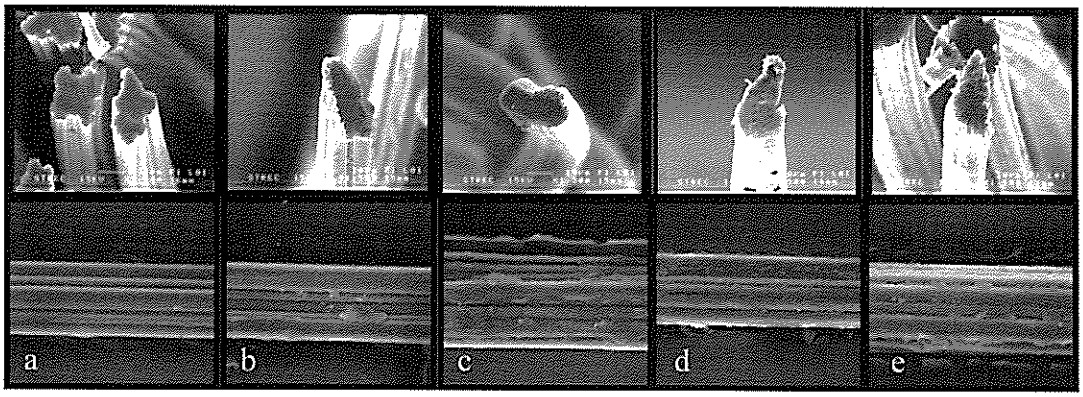

Figure 3. SEM photographs of cross-sections (top) and longtigudal sections of untreated rayon fiber (a); rayon fibres treated with 10 (b) and 40 (c) shots of nitrogen plasma; and with 10 (d) and 40 (e) shots of oxygen plasma.

change along the fiber surface which is possibly a result of heating effect. Therefore, it is expected that as the number of plasma shots increases, the fiber surface was increasingly heated. Consequently, the average diameters of treated fibers should be lower than that of the untreated one. However, the average diameters of oxygen plasma-treated fibers were similar to untreated one, but the average diameters of nitrogen plasma-treated fibers were higher than that of the untreated one (Table 1). This may be because plasma-treated rayon fibers can absorb higher amount of moisture than untreated fiber due to hydrophilic functional groups, which were present on the surface of plasma-treated fibers as previously mentioned. This moisture absorption can cause the swelling of the fibers. As a result, the diameters of the fibers increase. In the case of oxygen plasma-treated fibers, the swelling effect and heating effect were equivalent; consequently, the diameters of untreated and treated fibers were comparable. On the other hand, for nitrogen plasma-treated fibers, the swelling effect was dominant; therefore, the diameters of treated fibers were higher than that of untreated fiber.

Table 1. Diameters of untreated and plasma-treated rayon fibers.

Type of rayon fiber	Diameter (μm)	
	Nitrogen	Oxygen
Untreated	20.94±2.48	20.94±0.15
Treated with 10 plasma shots	25.58±2.48	20.87±0.15
Treated with 40 plasma shots	24.78±2.48	20.65±0.15

The effects of plasma treatment on linear density of rayon fibers measured using ASTM D1577 are shown in Figure 4. This fiber characteristic is used to determine the weight of fibers that may change during surface modification. It is shown in the form of weight per length at 9,000 meters (Denier). It can be seen that linear densities of plasma-treated rayon fibers, especially the nitrogen-plasma treated ones increase as the number of plasma shots increases. This is expected as the linear densities of oxygen plasma-treated fibers were similar to the untreated one, and those of nitrogen plasma-treated fibers were higher than that of the untreated one due to the moisture absorbed by hydrophilic groups formed on the fiber surface.

Figure 5 shows the tenacity of untreated and plasma-treated rayon fibers measured according to ASTM D2256. It can be seen that the tenacity of all treated rayon fibers tends to be lower than that of the untreated fiber. This may be due to plasma

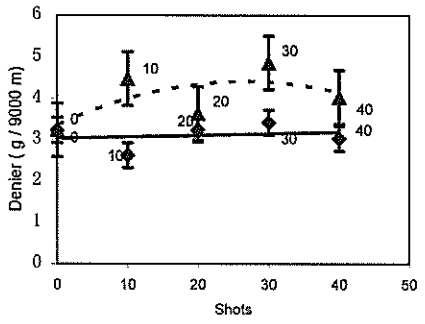

Figure 4. Linear densities of untreated and plasma-treated rayon fibers. ▲ Rayon (N); ♦ Rayon (O); dash line, Rayon (N); solid line, Rayon (O)

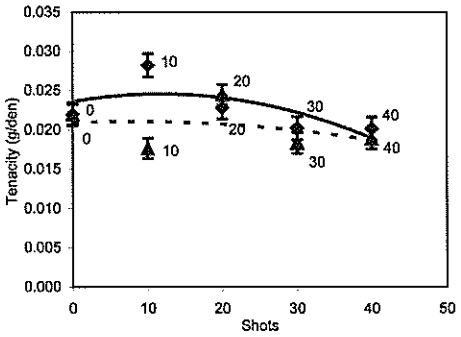

Figure 5. Tenacity of untreated and plasma-treated rayon fibers. ▲ Rayon (N); ♦ Rayon (O); dash line, Rayon (N); solid line, Rayon (O)

heating of the fiber as previously discussed. This heating effect can lower the molecular weights of rayon molecules resulting in lower tensile strength. Therefore, the tenacity of plasma-treated fibers should decrease with increasing the number of plasma shots. However, a slight increase in tenacity was observed when 10, 20 and 30 plasma shots in the case of oxygen plasma treatment and 20 plasma shots in the case of nitrogen plasma treatment were applied. This suggests that another factor acts in contrast to heating effect. Figures 1 and 2 indicate the formation of hydrophilic groups on the fiber surface after plasma treatment. These hydrophilic groups can form strong intermolecular bonds such as hydrogen bonds; as a result, the tenacity of plasma-treated rayon fibers should increase with increasing the number of plasma shots. Therefore, when heating effect dominated, the tenacity of plasma-treated fiber is lower than that of the untreated one (Fig. 5). On the other hand, when enough strong intermolecular bonds were formed, even plasma heated rayon molecules and lowered their molecular weights, the tenacity of plasma-treated fiber is higher than that of the untreated one.

CONCLUSION

The above results indicated that the surface of rayon fibers can be modified by pulsed plasma generated from a theta pinch device. The morphology and properties of plasma-treated rayon fibers were affected by several parameters including the type of gases and the number of plasma shots. While nitrogen plasma-treated fibers had higher moisture content, linear density and diameter but lower tenacity than the untreated fiber, oxygen plasma-treated fibers exhibited similar linear density and diameter but higher moisture content and tenacity than the untreated one. This was due to different types and amounts of hydrophilic functional groups formed on the fiber surface as confirmed by FT-IR spectroscopy.

The work reported in this paper is an initial attempt of using the theta pinch plasma for surface modification of fiber. Although the results are encouraging, further work is needed to raise the condition of the plasma to an electron temperature of perhaps around 10 eV in order to enhance the effect of particle interaction with material surface. One possibility is to operate the theta pinch at lower pressure and it may be possible to introduce etching effect into the treatment of fiber surface.

Acknowledgements – The authors would like to thank Num Rung Rayon Co., Ltd. for research material, Asian African Association for Plasma Training (AAAPT), Plasma Research Laboratory, University of Malaya, Plasma Research Laboratory, Department of Physics, Chulalongkorn University, Center of Excellence in Textiles, Department of Materials Science and Scientific Technological Research Equipment Centre (STREC), Chulalongkorn University for instrumental support. The authors would also like to acknowledge Recycling Technologies and Degradable Materials Research and Development Unit and Graduate School, Chulalongkorn University for their financial support.

REFERENCES

1. Kim B.C. (2000) Modification of Nylon. In: *Polymer Modification: Principles, Techniques and Applications* (ed. J.J. Meister). Marcel Dekker, New York.
2. Kan C.W, Chan K., Yuen C.W.M. and Miao M.H. (1998) *J. Mater. Proc. Technol.* **83:**180-184.
3. Poletti G., Orsini F., Raffaele-Addamo A., Riccardi C. and Selli E. (2003) *Appl. Surf. Sci.* **219:** 311-316.
4. Cioffi M.O.H., Voorwald H.J.C. and Mota R.P. (2003) *Mater. Charact.* **50:** 209-215.
5. Ueno S., Nomura H., Hashizume S. and Nishide T. (1986) United States Patent.
6. Ferrero F. (2003) *Polymer Testing* **22:** 571-578.

7. Riccardi C., Barni R., Selli E., Mazzone G., Massafra M., Marcandalli R. and Poletti G. (2003) *Appl. Surf. Sci.* **211:** 386-397.
8. Iriyama Y., Yasuda T., Cho D.L. and Yasuda H. (2003) *J. Appl. Polym. Sci.* **39:** 249-264.
9. Rahel J., Simor M. and Emak M. (2003) *Surf. Coat Technol.* **172:** 604-608.
10. Wei Q.F. (2004) *Mater. Charact.* **52:** 231-235.
11. Simor M., Rahel J. and Emak M. (2003) *Surf. Coat Technol.* **172:** 1-6.

Journal of Science and Technology in the Tropics (2007) **3:** 27-32

Low-cost hydrocarbon templated sol-gel synthesis of functional nanoporous silica xerogel

M. Halina [1], Y. M. Ambar [2] and S. Ramesh [3]
[1]Nanostructured Materials Laboratory and [3]Ceramics Technology Laboratory,
College of Engineering, University Tenaga Nasional, Km 7, Jalan Kajang-Puchong,
43009 Kajang, Selangor, Malaysia
[2]School of Science and Food Technology, Universiti Kebangsaan Malaysia,
43600 UKM-Bangi, Malaysia
(Email: halina@uniten.edu.my)

Abstract Nanoporous silica xerogels were successfully synthesized without using commercial surfactant in a direct synthesis method by a modified sol-gel route employing acoustic emulsification technique. In the present work, commercially available ionic surfactants were substituted by locally produced palm oil and its hydrocarbon-based derivatives as templates. Acoustic emulsification during the synthesis enabled the formation of stable precursor sols with relatively narrow oil droplet size distributions. The silica xerogels exhibited relatively high specific surface area of ca. 270 m^2/g to 600 m^2/g. The pore volume observed was ca. 0.8 to 1.5 mL/g. The nanoporous channel networks were of disordered wormhole-like structure and the morphologies were of monodispersed spherical particles with diameter ranging from ca. 50 nm to 150 nm. The functionalization of silica xerogels for pH sensing was evaluated and the results showed that the silica exhibited stable absorbance at different pH values for more than 5 cycles.

Keywords surfactant-free – nanoporous – pH sensing – xerogels – fatty alcohols

INTRODUCTION

Nanoporous silicas with pore sizes from 2 nm to 50 nm have high surface areas and pore volumes which make them favourable for several applications. Such applications include catalysis, catalyst supports, adsorbents for hazardous gases, gases sensors, drug delivery system, nanodevices and nanoelectronics. These applications are achieved by functionalizing the silanols (Si-OH) groups on the pore surface or in the silica framework with the desired functional groups [1-5].

Another important application of nanoporous silicas is as hard templates in the synthesis of nanoporous films. In a typical process, a multilayer nanoporous film is obtained upon the removal of silica nanoparticles after crosslinking had occurred [6]. Additionally, metal oxides are also synthesized using the nanocasting method employing porous silica as hard template over the soft template (surfactant) method [7]. By employing nanoporous silica as hard template in the synthesis of metal oxides, the usage of surfactants is eliminated in the synthesis process and the amount of liquid by-products is substantially reduced. Consequently, the production of metal oxides becomes more economical and environmental-friendly [8]. Moreover, the nanoporous silica contains high open-ended pores and more silanol groups (Si-OH) on the pore surface. These features will enhance the impregnation process of the precursor solutions containing metal ions for the synthesis of the designated metal oxides [9].

In recent years, ultrasonic treatment has been employed in the preparation and functionalizations of nanostructured materials [10-12]. Acoustic emulsification enables the preparation of stable emulsions without the addition of surface-active materials.

The conventional method of preparing nanoporous silica xerogel materials involves the usage of surfactants with ionic and non-ionic head-

groups as porous structure directing agents [13]. Commercially available surfactants generally used in the syntheses of nanostructured materials are designer chemicals that are expensive and toxic to the environment and human. Thus, the scale-up production for industrial usage is difficult to achieve.

The present report deals with the synthesis of nanoporous silica xerogel by substituting commercial surfactants with locally produced oil-based hydrocarbons and their derivatives to give soft impact to the environment as well as to keep the cost of synthesis low. In this process, stable precursor sols were achieved by acoustic emulsification. In addition, hydrothermal aging treatment was not necessary to obtain relatively porous materials. Then, we functionalized the silica xerogel with phenol red for pH sensing properties and the effectiveness of the materials was evaluated.

MATERIALS AND METHODS

Synthesis of silica xerogels

The syntheses were carried out by a modified sol-gel method reported by Schumacher *et al.* [14], based on hydrolysis and condensation-polymerizations of TEOS as the silica precursor in various compositions of oil-in-water emulsion formed by acoustic emulsification. The syntheses were carried out at room temperature. The oils used in this study were palm oil and palm oil-derived fatty alcohols with carbon chain of C8 to C12, respectively.

In a typical synthesis procedure, oil and co-solvent of ethanol were added to deionized water and subjected to acoustic emulsification at predefined time period. Then, silica precursor of TEOS was added dropwise to the solution mixture containing base catalyst under ultrasonic treatment. The final composition of the gel was 1:5:231 parts of TEOS:oil:water. In order to investigate the effect of co-solvent, the ratio of co-solvent to water was varied at 1:2 and 1:5. Then, to study the effect of oil concentration on the properties of the materials, the ratio of oil to water in the emulsion was also varied. The solution mixture was stirred at room temperature under ambient conditions for 24 h. After that, the pH of the solution was adjusted using an organic acid to obtain gelation. The resulting gel mixture was filtered, washed and dried at 373 K to obtain as-synthesized material. The samples were calcined at 823 K for more than 5 h to obtain the calcined materials. These samples were labeled according to processing conditions (Table 1).

Table 1. Sample details and preparation conditions.

Sample code	Length of carbon chain in oil	Synthesis condition	Co-solvent : water ratio (v/v)
ULSF-4	C10	0.04 M	1 : 2
ULSF-6	C8	0.02 M	1 : 5
ULSF-8	C12	0.04 M	1 : 5
ULSF-9	C10	0.04 M	1 : 5
ULSF-10-PR	C8	0.04 M	1 : 5

Functionalizations of silica xerogels

In this work, we doped the sol-gel mixture with phenol red (PR) 'one-pot' co-condensation method. In this procedure, phenol red and TEOS were added simultaneously to the solution mixture as described earlier. After stirring for 24 h, the pH of the solution was adjusted until gelation occurred. The resulting gel was filtered, washed and dried, and the solvent extracted using ethanol for several times to remove organic moieties. This sample was labeled as ULSF-10-PR (Table 1).

Characterizations

Structural characterizations were done on as-synthesized and calcined materials. X-ray diffraction (XRD) analyses were performed using a Rigaku Geiger-Flex at 30 kV and 20 mA at 2θ angle ranging from 1.5° to 70°. Nitrogen sorption measurements were done by Quantachrome NOVA 1200e at liquid nitrogen temperature of 77 K. Specific surface area of the synthesized particles was estimated using the Brunauer-Emmet-Teller (BET) method and the pore volume was estimated based on standard non-porous silica, Aerosils 200. Solid state ^{29}Si NMR and ^{13}C NMR spectra were measured using Bruker AV400 spun at 3 kHz and 1000 times scan. Pore channel networks were studied by bright field transmission electron microscopy (TEM) using a Philip Tecnai operating at an acceleration voltage of 200 kV. The particles morphology was observed using a LEO 1400VP scanning electron microscope (SEM) operating at an acceleration voltage of 20 kV.

Absorbance measurements were made using a UV-VIS double beam spectrophotometer Shimadzu UV-1650PC at 560 nm. Standard buffers of pH 4 (acetic acid-acetate), 7 (phosphates), 9 and 10 (borate and carbonate) were used to measure the effectiveness of the functionalized silica xerogel. The concentration of phenol red in the buffer solution was 1.03×10^{-3} M. Absorption spectra were measured in a standard cuvette at room temperature for more than 5 cycles.

RESULTS AND DISCUSSION

Phase and nitrogen sorption analyses

The XRD analysis (not shown) on calcined silica xerogels showed a broad peak centered at $2\theta = 22°$, suggesting that the materials were of amorphous nature. The absence of pronounced peaks at lower angle also indicated that the pores were of disordered wormhole-like structure due to the absence of self-assembled micelles as typically observed in microemulsion using commercial surfactant [15].

Nitrogen adsorption isotherms of calcined samples are shown in Figures 1 to 3. The BET equation was applied to the region of monolayer adsorption and the t-plot method was used to estimate the total pore volume while the median pore diameter was estimated from maximum value of BJH pore size distributions (Table 2).

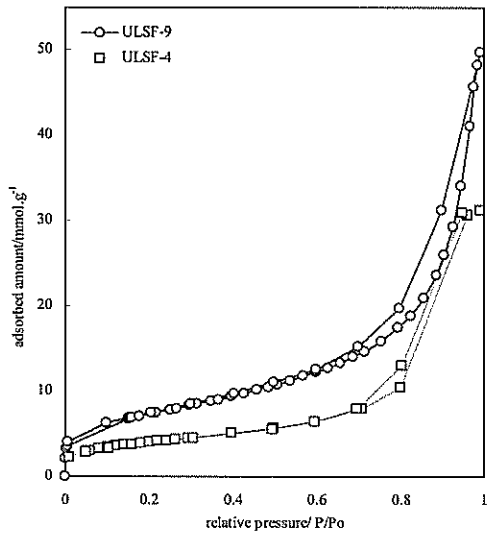

Figure 1. Nitrogen adsorption isotherms of calcined samples (ULSF-4 and ULSF-9) using C10 fatty alcohols as template.

Table 2. Pore characteristics of calcined and solvent extracted silica xerogels.

Sample code	Pore size [c] (nm)	Specific surface area [a] (m^2/g)	Total pore volume b (mL/g)
ULSF-4	11	319	1.0
ULSF-6	10.8	305	0.94
ULSF-8	10	494	1.1
ULSF-9	9.5	600	1.5
ULSF-10-PR	7.4	495	0.8

[a] By BET method, [b] By t-plot method, [c] Maximum value by Barret-Joyner-Halenda (BJH) method.

Nitrogen isotherms of silica xerogels prepared with different co-solvent/water ratio of 1:2 (ULSF-4) and 1:5 (ULSF-9) shown in Figure 1 exhibited Type IVa and Type IIb, respectively in the IUPAC (International Union of Pure and Applied Chemistry) classifications similar to MCM-type mesoporous silica materials [16]. These results indicated the successful formation of mesoporous silica xerogels. Type IIb isotherm is generally associated with aggregates of plate-like particles which therefore possess non-rigid slit-shaped pores [17].

The BET surface area increased approximately two-fold from 319 m^2/g to 600 m^2/g while the pore volume also increased from 1.0 mL/g to 1.5 mL/g as the co-solvent ratio was increased (Table 2). This was probably due to the oil used as template, which was more dispersed in the continuous water phase as the co-solvent was increased. As a result, more oil droplets that were finer in size could be formed and condensation-polymerization of the silica precursor occurred on the surface of these oil droplets. The increment also suggested that the oil dispersed in continuous water phase in the oil-in-water emulsion played the role similar to the micelles from conventional surfactants where the hydrolysis and condensation-polymerization of TEOS occurred on the surface of the oil drops. The estimated pore volume also increased accordingly together with the increment of BET surface area.

Nitrogen isotherms of calcined silica xerogels prepared from C8 fatty alcohol (ULSF-6) and solvent-extracted functionalized silica xerogels prepared from C8 fatty alcohol (ULSF-10-PR) are shown in Figure 2. Both samples exhibited Type IVa in the IUPAC classification with a distinct plateau at

Editorial

R&D culture in Science and Technology needs to be nurtured, encouraged and supported. The rapid development of higher education in Malaysia provides the appropriate environment and stimulus for R&D activities to develop, expand and thrive.

The foundation for such a culture is the strong desire to be original and to achieve excellence based on scholarship and creativity. It would be desirable to develop the ability of our scientific researchers to communicate effectively in print as well as orally.

Malaysians have demonstrated their capability in original research especially in physical sciences, biomedical sciences, science and technology applied to industrial solutions in rubber and oil palm industries.

We look forward to our current researchers to meet the challenges in the areas of renewable energy and environmental issues especially in the tropical region. We hope that the solutions in the form of research findings will be published in JOSTT.

Academician Tan Sri Datuk Dr Augustine S. H. Ong
Co-Chairman, Editorial Board

higher relative pressure region indicating a delayed condensation of the adsorbate in the mesopores. The hysteresis loop is of Type H1 but is relatively narrow, almost parallel adsorption-desorption step usually given by adsorbents with an open-ended tubular pores such as MCM-type materials [17]. However, the functionalized silica xerogels ULSF-10-PR exhibited Type H3 hysteresis loop in accordance to the IUPAC classification, suggesting that the pores were slit-shaped and the particles were of platy agglomerations.

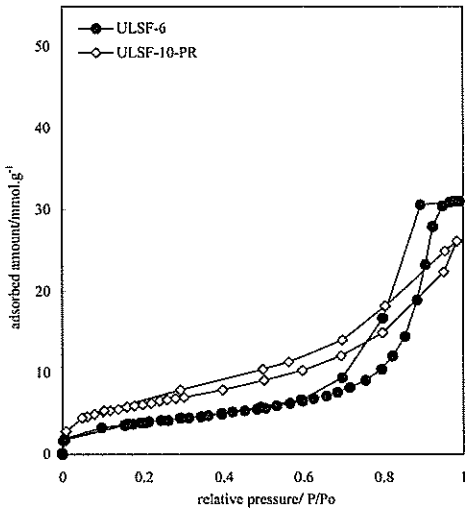

Figure 2. Nitrogen adsorption isotherms of calcined samples (ULSF-6 and ULSF-10-PR) using C8 fatty alcohol as template.

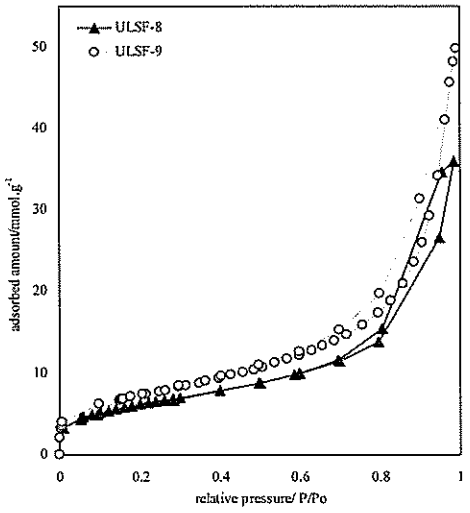

Figure 3. Nitrogen adsorption isotherms of calcined samples using C12 (ULSF-8) and C10 (ULSF-9) fatty alcohol as template.

The nitrogen adsorption isotherms of calcined silica xerogels prepared with oil derivatives with different carbon chain length C12 (ULSF-8) and C10 (ULSF-9) as template are shown in Figure 3. Silica xerogels prepared from higher carbon chain length (ULSF-8) exhibited lower BET surface area of 494 m^2/g compared to 600 m^2/g for silica xerogels prepared from C10 as template (ULSF-9). The pore volume was also higher for ULSF-9 at ca. 1.5 mL/g compared to ULSF-8 at 1.1 mL/g (Table 2).

The isotherms exhibited by ULSF-8 are of Type IVa and the distinct plateau observed at higher relative pressure (Fig. 3) is typical of mesoporous materials. On the other hand, ULSF-9 displayed Type IIb isotherms which are typical of platelets agglomeration possessing slit-shape pores. The results suggested that the emulsion containing fatty alcohols with long carbon chain C12 had the tendency to form mesoporous materials having open-ended mesopores due to the stability of the oil droplets caused by the long hydrophobic carbon chain during the synthesis similar to that observed for conventional surfactant micelles [15, 17].

Particles morphology

The representative SEM images of calcined xerogels ULSF-4 and ULSF-6 are shown in Figure 4. In general, the calcined samples exhibited fine globular units of spherical agglomerations with particle diameters of less than 50 nm. Samples prepared from fatty alcohols with longer carbon chain exhibited larger particles probably due to the formation of bigger oil droplets in the emulsion by acoustic emulsification to enable the hydrolysis and condensation-polymerizations of the silica on their surface during the synthesis.

The TEM images of pore channel networks of as-synthesized and template-free (ULSF-10-PR) samples are shown Figure 5. The agglomerations of spherical particles consisted of finer globular units giving rise to slit-shaped pores and cylindrical pores as well as disordered wormlike structure in template-free functionalized silica xerogels prepared from palm oil without acoustic emulsification. However, the sample prepared from oil phase with a shorter carbon chain length of fatty alcohols formed disordered wormhole like structure that was almost cylindrical. Denser areas were observed which might be formed during the drying process of

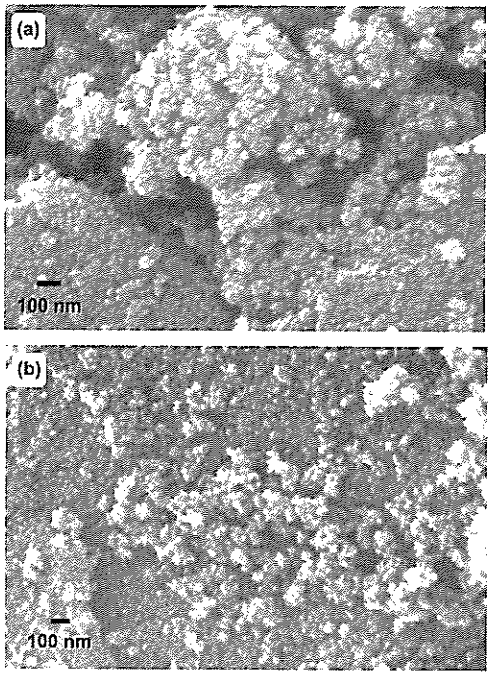

Figure 4. SEM images of calcined silica xerogels. (a) ULSF-4, (b) ULSF-6.

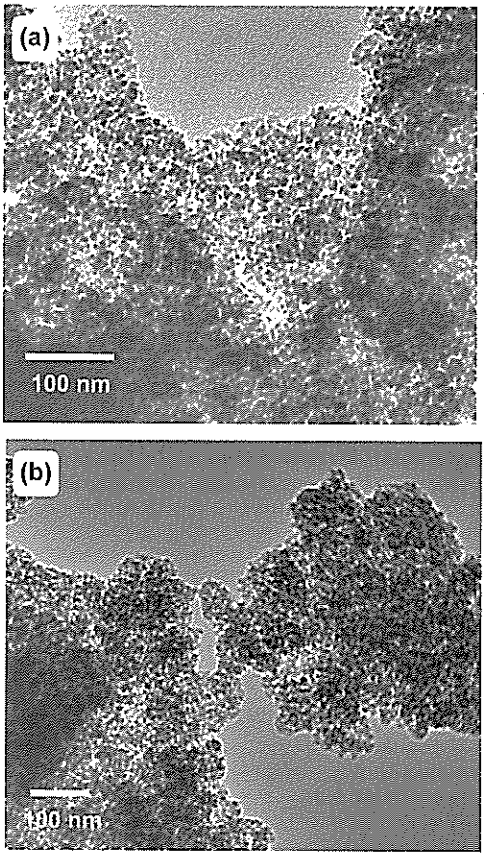

Figure 5. TEM images of (a) as-synthesized functionalized silica xerogel ULSF-10-PR and (b) template-free functionalized silica xerogel ULSF-10-PR.

the as-synthesized gel. Connecting pore windows were observed between the pores at certain areas indicating the occurrence of oil drops coalescence that caused bigger oil drops to form. Consequently, bigger pores and bigger particle diameters were obtained. The results showed that the substitution of commercial surfactant with locally produced palm oil and its hydrocarbon-based derivatives were beneficial in aiding the development of nanoporous structure with similar mechanism to that of MCM-type materials [15].

pH response spectra

The colour of the phenol-red functionalized silica xerogel (ULSF-10-PR) was yellow, but it changed to pink when in contact with buffer solution of pH 9 and pH 10. Very small amount of leaching of the dye was observed when the powder was dissolved in the buffer solution. Figure 6 shows the absorbance spectra of phenol-red doped silica gel of ULSF-10-PR in buffer solutions with different pH values. At low pH value, the absorbance maximum was observed at ca. 430 nm. However, as the pH value was increased, the peak disappeared completely while the peak at ca. 560 nm continued to increase. An isobestic point was observed at ca. 482 nm at higher pH of 9-10. This peak was observed due to the isobestic point of phenol red in the solution. No shift in the absorption peak at higher pH was observed indicating that the phenol-red maintained its stability in the adsorbed form in the ULSF-10-PR sample.

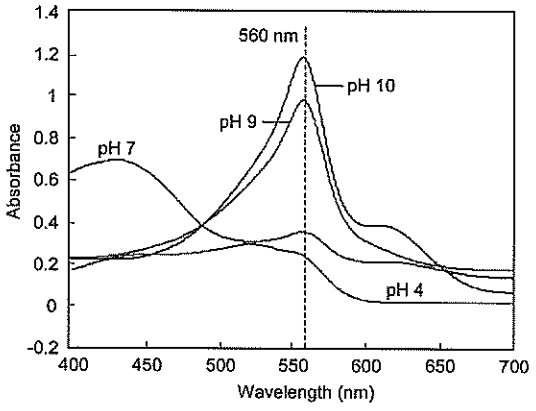

Figure 5. Absorption spectra of phenol red in ULSF-10-PR in buffer solutions of various pH ranging from 4-10.

CONCLUSION

Nanoporous silica xerogels with high surface area, high pore volume and fine spherical morphology with particle size ranging from ca. 50 to 150 nm were successfully synthesized using locally produced hydrocarbons and the derivatives of fatty alcohols employing acoustic emulsification. The oil droplets in the presence of co-solvent such as short-chain alcohols to act as dispersant behaved as template where the hydrolysis and condensation-polymerization of silica precursors could take place. Furthermore, the silica xerogels synthesized in this study exhibited properties that are suitable as support materials for pH sensing. Thus, it is envisaged that the silica xerogels have the potential for use in other fields such as removal of hazardous gases and this will be the subject of future study.

Acknowledgements–The authors gratefully acknowledge UNITEN for providing the seeding fund (J510010216).

REFERENCES

1. Fryxell G.E. (2006) The synthesis of functional mesoporous materials. *Inorganic Chemistry Communications* **9:** 1141-1150
2. Hubbe M.A., Rojas O.J., Lee S.Y., Park S. and Wang Y. (2007) Distinctive electrokinetic behavior of nanoporous silica particles treated with cationic polyelectrolyte. *Colloids and Surfaces A: Physicochemical and Engineering Aspects* **292:** 271-278.
3. Johnson-W.B., Zeinali M., Shaffer K.M., Patterson C.H., Charles P.T. and Markowitz M.A. (2007) Detection of organics using porphyrin embedded nanoporous organosilicas. *Biosensors and Bioelectronics* **22:** 1154-1162.
4. Cheng X., Liu S., Lu L., Sui X., Meynen V., Cool P., Vansant E.F. and Jiang J. (2007) Fast fabrication of hollow silica spheres with thermally stable nanoporous shells. *Microporous and Mesoporous Materials* **98:** 41-46.
5. Chong A.S.M. and Zhao X.S. (2004) Functionalized nanoporous silicas for the immobilization of penicillin acylase. *Applied Surface Science* **237:** 398-404.
6. Yan J., Wang A. and Kim D.-P. (2006) Preparation of ordered mesoporous SiC from preceramic polymer templated by nanoporous silica. *J. Phys. Chem. B.* **110:** 5429-5433.
7. Delahaye E., Escax V., El Hassan N., Davidson A., Aquino R., Dupuis V., Perzynski R. and Raikher Y.L. (2006) Nanocasting: using SBA-15 silicas as hard templates to obtain ultrasmall monodispersed γ-Fe_2O_3 nanoparticles. *J. Phys. Chem. B.* **110:** 26001-26011.
8. Smatt J.-H., Weidenthaler C., Rosenholm J.B. and Linden M. (2006) Hierarchically porous metal oxide monoliths prepared by the nanocasting route. *Chem. Mater.* **18:** 1443-1450.
9. Fajula F., Galarneau A. and Di Renzo F. (2005) Advanced porous materials: new developments and emerging trends. Microporous and Mesoporous Materials **82:** 227-239.
10. Al-Kaysi R.O., Muller A.M., Ahn T.-S., Lee S. and Bardeen C.J. (2005) Effects of sonication on the size and crystallinity of stable zwitterionic organic nanoparticles formed by reprecipitation in water. *Langmuir* **21:** 7990-7994.
11. Sakai T., Sakai H. and Abe M. (2002) Dimpled polymer particles prepared by a single-step method in an acoustic field. *Langmuir* **18:** 3763-3766.
12. Xing Y., Li L., Chusuei C., Hull R.V. (2005) Sonochemical oxidation of multiwalled carbon nanotubes. *Langmuir* **21:** 4185-4190.
13. Wang X., Li W., Zhu G., Qiu S., Zhao D. and Zhong B. (2004) Effects of ammonia/silica molar ratio on the synthesis and structure of bimodal mesopore silica xerogel. *Microporous and Mesoporous Materials* **71:** 87-97.
14. Schumacher K., Grun M. and Unger K.K (1999) Novel synthesis of spherical MCM-48. *Microporous and Mesoporous Materials* **27:** 201-206.
15. Matsumoto A., Misran H. and Tsutsumi K. (2004) Adsorption characteristics of organosilica based mesoporous materials. *Langmuir* **20:** 7139-7145.
16. Beck J.S., Vartulli J.C., Roth W.J., Leonowicz M.E., Kresge C.T., Schmitt K.D., Chu C.T.-W., Olson D.H., Sheppard E.W., McCullen S.B., Higgins J.B. and Schlenker J.L. (1992) A new family of mesoporous molecular sieves prepared with liquid crystal templates *J. Am. Chem. Soc.* **114:** 10834-10843.
17. Matsumoto A., Chen H., Tsutsumi K., Grün M. and Unger K. (1999) Novel route in the synthesis of MCM-41 containing framework aluminum and its characterization. *Microporous and Mesoporous Materials* **32:** 55-62.

Journal of Science and Technology in the Tropics (2007) **3:** 33-38

Extraction of *Elaeis oleifera* mesocarp and kernel oils using supercritical carbon dioxide

Harrison Lik Nang Lau[1,2], Yuen May Choo[1], Ah Ngan Ma[1] and Cheng Hock Chuah[2]
[1]Malaysian Palm Oil Board, Bandar Baru Bangi, 43000 Kajang, Selangor, Malaysia
[2]Department of Chemistry, Faculty of Science, University of Malaya,
50603 Kuala Lumpur, Malaysia
(Email: harrison@mpob.gov.my)

Received 01.11.2006; accepted 10.01.2007

Abstract The extractions of mesocarp and kernel oils from *Elaeis oleifera*, another oil palm species using SC-CO_2 were studied. The temperatures and pressures used were 40°C, 60°C and 80°C, and 18 MPa, 24 MPa and 30 MPa, respectively. The mesocarp and kernel oils extracted were found to be highly unsaturated with total unsaturations of 79% and 32% respectively. The mesocarp oil is rich in minor components such as carotenes, vitamin E, sterols and squalene with concentration of 2-3 times that of the commonly cultivated oil palm species (*Elaeis guineensis* or better know as *Tenera*). The optimum condition for the mesocarp oil extraction was at 80°C and 24 MPa. Fatty acids compositions of mesocarp and kernel oils of *E. oleifera* were similar respectively to the hexane extracted oils. This clean and environmental friendly extraction technology has been demonstrated to extract more than 95% of oils from both mesocarp and kernel of the *E. oleifera*.

Keywords *Elaeis oleifera* – supercritical carbon dioxide – vitamin E – sterols – carotenes

INTRODUCTION

Elaeis oleifera (or Melanococca) is an oil palm species that originated from South and Central America. Unlike the commercial oil palm, *Elaeis guineensis* (Tenera) planted in Malaysia and Indonesia, *E. oleifera* has not been commercially exploited because of its low oil yield. Choo and Basiron [1] reported that only 0.5 tonne of oil is produced from every hectare of plantation per year. However, the potential revenue from *E. oleifera* oil per hectare per year is almost 10 times that of *Tenera* due to the unique characteristics of the oil, which has been found to contain higher levels of unsaturated fatty acids (higher iodine value) and phytonutrients. *Tenera* palm oil has about 50:50 ratio of saturated and unsaturated fatty acids content whereas the unsaturation in *E. oleifera* oil is >75%. The *E. oleifera* oil has higher level of carotenes (4300-4600 ppm), vitamin E (800-1500 ppm in terms of tocopherols and tocotrienols) and phytosterols (3500-4000 ppm) which are higher (5, 2 and 3 times respectively) than those of commercial palm oil [1]. Thus, the oil can provide a good source of these phytonutrients for pharmaceutical and nutraceutical applications.

The commercial extraction of oil from *E. oleifera* has not been fully established; one reason is its thin mesocarp, which limits its oil extraction rate using normal screw press. In the laboratory, hexane has been used to recover the oil for research purposes. However, this extraction method poses environmental and health concerns. Thus, supercritical fluid extraction using carbon dioxide (SC-CO_2) was investigated as an alternative method for recovery of this high value *E. oleifera* oil.

In the last two decades, supercritical fluid extraction technology has been extensively evaluated as an alternative method over screw press and solvent extraction which have been used in oilseed extraction plants. Researchers have reported on the SC-CO_2 extraction of cottonseed

oil [2], degumming and refining of soybean oil [3], concentration of vitamin E in deodorizer distillate of soybean oil [4], extraction of corn oils [5], extraction of phospholipids in soybeans [6] and many other applications. Some work related to *E. guineensis* palm oil using SC-CO_2 have also been published, but not on *E. oleifera* palm species [7,8,9].

In this study, the extraction efficiency of *E. oleifera* palm oil using SC-CO_2 and the minor components in the oil were investigated. The fatty acid composition (FAC) of kernel oil was also reviewed.

EXPERIMENTAL PROCEDURES

Materials

Fresh fruit bunches (FFB) of *E. oleifera* were obtained from Malaysian Palm Oil Board (MPOB) Kluang Station (Johor, Malaysia) and Hulu Paka Station (Terengganu, Malaysia). The FFB was sterilized using autoclave at 150°C for one hour. The fruitlets were detached from the stalk and the mesocarp was peeled off from the nut with a stainless steel blade. The mesocarp was then dried in an oven at 60°C until a constant weight was obtained. The dried mesocarp was ground into pieces of 1-3 mm lengths, sealed under nitrogen and stored at –5°C. The oil content in the bunch was determined by solvent extraction using hexane. Concurrently, the mesocarp was subjected to SC-CO_2 extraction and comparison was made between the two types of oil obtained by different extraction methods. The nut of *E. oleifera* fruit was cracked to obtain the kernel and the kernel was ground (1-3 mm i.d.) before being subjected to SC-CO_2 extraction and hexane extraction for 6 hours.

Reagents and chemicals

CP-grade CO_2 with 99.995% purity was purchased from Malaysia Oxygen Berhad (Selangor, Malaysia). Myristic acid (14:0), palmitic acid (C16:0), stearic acid (C18:0) and oleic acid (C18:1), monopalmitin, 1,2– and 1,3–dipalmitin and tripalmitin, with purities of 99%; β–sitosterol (95%); campesterol (98%); stigmasterol (95%) and cholesterol (99%) were purchased from Sigma Aldrich Inc. (St. Louis, MO). Silylation reagent N,O–*Bis* (trimethylsilyl) trifluoroacetamide with 1% trimethylchlorosilane (BSTFA) and methylation agent sodium methylate solution were purchased from Fluka Chemicals (Bushs, Switzerland). All solvents of chromatographic and analytical grade were purchased from Merck (Darmstadt, Germany).

SC-CO_2 apparatus and extraction procedure

The SC-CO_2 extraction system was designed by Jasco, Japan (Model CO-960) complete with a column oven (Jasco CO-960), an intelligent positive displacement HPLC pump (Jasco PU-980), a digital back-pressure regulator (Jasco 880-81) and an extraction vessel (Thar Designs, Inc.). The CO_2 chiller was purchased from Polyscience (Pittsburg, PA). The co-solvent pump used was Waters 510 HPLC pump (Milford, MA).

The mesocarp (25.0 g) was weighed accurately into a 100 mL high-pressure extraction vessel. The extraction temperatures were programmed at 40°C, 60°C and 80°C with pressures of 180 MPa, 240 MPa and 300 MPa, respectively. The extractor was equilibrated for 30 minutes and liquid CO_2 at 5.0 mL/min was continuously pumped through the vertical vessel from bottom to top. The solute-solvent stream was depressurised by expanding through a heated needle valve to atmospheric pressure while the oil was collected in a receiver. The sample was kept at –5°C prior to analyses. The extractions were carried out in triplicates to ensure reproducibility.

Analyses

The oil samples was analysed according to MPOB Test Methods for total carotene content [10]. The free fatty acids (FFA), monoacylglycerols (MAG), diacylglycerols (DAG), triacylglycerols (TAG), phytosterols and squalene were determined using Hewlett-Packard GC-FID (5890 series II, Agilent Technologies, Palo Alto, CA) fitted with a capillary column (15 m × 0.32 mm i.d., SGE, Austin, TX) coated with 5 % phenyl-95% polysilphenylene-siloxane [11]. The fatty acids composition (FAC) was determined using PerkinElmer GC-FID (AutoSystem XL, Shelton, CT) fitted with fused silica column (30m × 0.53 mm i.d.; 0.5um film) (SGE, Ringwood, Australia). Sodium methylate (0.3 mL) and hexane (1.0 mL) were added to 0.03 g of sample. The mixture was homogenised using vortex and 1.0 uL of sample (bottom layer) was injected into GC with split ratio of 1:100. The vitamin E content was analysed by using HPLC-

Fluorescence Detector (Agilent Technologies) with a silica column (5 µm; 150 mm × 4.6 mm i.d., Zorbax, Aligent Technologies) eluted by using 1.0 mL/min of *n*-hexane/THF/IPA (93.9:5.7:0.4, v/v/v). The excitation and emission wavelengths were set at 292 and 326 nm, respectively. All analyses were carried out in triplicates.

RESULTS AND DISCUSSION

Oil extraction rate

The oil yield obtained from hexane extraction was 28% based on dry basis. The total lipids recovery using SC-CO_2 was 95% based on hexane extractable matter. The extraction rate of a substance in SC-CO_2 is directly dependent on the extraction temperature and pressure. This is clearly shown in the recovery of *E. oleifera* oil (Fig. 1). The oil was readily extracted at any temperature and pressure using SC-CO_2 but a higher extraction rate was obtained at higher pressure for any given temperature. For instance at 80°C, the oil was recovered at 0.0128 g/min at 30 MPa, 0.0083 g/min at 24 MPa and 0.001 g/min at 18 MPa. A longer extraction time is required to achieve similar recovery under lower operating pressure because the density of SC-CO_2 generated is lower, which gives milder solvating and diffusivity power. The solubility of oil is greatly affected by the extraction pressures.

At higher operating pressure (e.g. 30 MPa), temperature does not give significant effect on the extraction rate of *E. oleifera* oil. However, at lower pressure of 18 MPa, the recovery was significantly influenced by the operating temperature. Higher oil extraction rate was observed at lower temperature as compared to higher temperature (Fig. 1). The oil extraction rate increased drastically from 0.001 g/min at 80°C to 0.0049 g/min at 60°C and 0.011 g/min at 40°C. The observation can be explained as follows: the density of SC-CO_2 at lower pressure (e.g. 18 MPa) changes notably by elevation of temperature whereas at higher pressure, the density changes of SC-CO_2 at different temperatures do not affect much the oil solubility as its solvating power is high enough to extract oil from its matrix.

For this application, the design pressure for a commercial plant of 24 MPa and temperature of 40°C is recommended as it gives similar extraction rate as 30 MPa. However, design pressure at 18 MPa can be considered if more vessels in parallel are to be built to compensate for the loss in extraction time for similar working capacity.

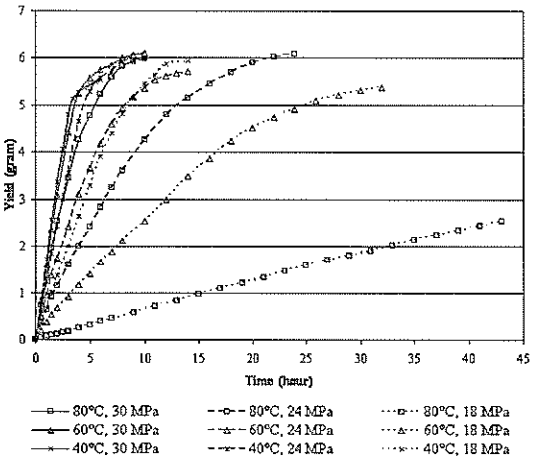

Figure 1. Recovery of oil from *E. oleifera* using SC-CO_2.

Glycerides and FA composition of *E. oleifera* palm oil

The acylglycerols compositions of the *n*-hexane and SC-CO_2 extracts are shown in Table 1. The FFA content of the *E. oleifera* oil was <0.5% due to the freshness of FFB that was received. Monoacylglycerols were not detected in both oils and very low amounts of diacylglycerols (<3.0%) were detected.

The FAC of *E. oleifera* palm oil showed that the *E. oleifera* oil was high in mono- and di-unsaturated C18 fatty acids (Table 2) which was of 30% more unsaturation than *Tenera* palm oil. The ratio of 16:0, 18:1 and 18:2 fatty acids was 1.0:2.9:1.0 and these fatty acids accounted for 95% of the total fatty acids. The percentage of total unsaturation and saturation were 80.8% and 19.2%, respectively.

Table 1. Free fatty acids and acylglycerols composition of *E. oleifera* Mesocarp oil.

Extraction method	Free Fatty Acids and Acylglycerols Composition of *E. oleifera* Mesocarp Oil (%)			
	FFA	MG	DG	TG
n-hexane	0.17 – 0.19	ND	1.70 – 1.86	96.53 – 97.95
SC-CO_2	0.27 – 0.30	ND	2.23 – 2.51	96.58 – 97.22

Note: ND is not detected; FFA, free fatty acids; MG, monoglycerides; DG, diglycerides; TG, triglycerides.

Table 2. Fatty acids composition of *E. oleifera* mesocarp oil.

Carbon chain length	Percentage (%)		
	Hexane extracted *E. oleifera* mesocarp oil	SC-CO_2 extracted *E. oleifera* mesocarp oil	*E. guineensis* mesocarp oil[a]
1. 12:0	0.01 – 0.02	0.01 – 0.02	0.1 – 0.4
2. 14:0	0.04 – 0.05	0.32 – 0.36	1.0 – 1.4
3. 16:0	19.1 – 19.3	19.2 – 19.6	40.9 – 47.5
4. 16:1	1.1 – 1.3	1.3 – 1.5	0 – 0.6
5. 18:0	0.7 – 0.9	0.9 – 1.1	.8 – 4.8
6. 18:1	55.1 – 57.5	55.4 – 57.4	36.4 – 41.2
7. 18:2	19.1 – 19.7	19.1 – 21.2	9.2 – 11.6
8. 18:3	0.8 – 0.9	0.9 – 1.1	0 – 0.5
9. 20:0	1.0 – 1.2	0.8 – 0.9	0 – 0.8

[a] Data obtained from *Pocketbook of Palm Oil Uses* [18].

Table 3 shows the vitamin E content of *E. oleifera* palm oil with α-tocopherol (34-38%) and γ-tocotrienol (55-60%) being the major ones. Less than 10% of the constituents were found to be α- and δ- tocotrienols. The concentration of vitamin E in *E. oleifera* palm oil was 1,000 ppm to 1,400 ppm. No significant differences in vitamin E content were found between *n*-hexane and SC-CO_2 extracted oils. However, the vitamin E profile of *E. oleifera* oil is a little different from the commercial *Tenera* palm oil. The total tocotrienols content of *E. oleifera* was slightly lower compared to *Tenera* palm oil which is about 70-80% of tocotrientols of total vitamin E [12].

The total carotene content of the *E. oleifera* palm oil obtained from *n*-hexane and SC-CO_2 extraction were 2,786 ppm and 2,317 ppm respectively. Most carotenes were extracted at the later stage of extraction using SC-CO_2 as they are strongly adhered to the fibrous materials. Owing to the limited solvating power of SC-CO_2 as compared to organic solvent, gummy materials such as phospholipids were not extracted with the oil [13]. The carotenes content of *E. oleifera* was 3 times higher than *Tenera* palm oil. Thus, *E. oleifera* palm oil can be a good source of carotenes (pro-vitamin A) especially for individuals facing vitamin A deficiency problem.

Like other oil palm species, β-sitosterol was the major sterol found in the *E. oleifera* palm oil (Table 4). It accounted for 65-70% of the total sterols followed by 17-20% of campesterol and 11-13% of stigmasterol. Cholesterol was not detected (GC detection limit of <0.001%) in both hexane and SC-CO_2 extracted oils.

Squalene was detected in the *E. oleifera* palm oil at 1,200 ppm to 1,300 ppm. The concentration of

Table 3. Vitamin E content of *E. oleifera* mesocarp oil.

Extraction method	Vitamin E isomers of *E. oleifera* mesocarp oil (%)				
	α-Tocopherol	α-Tocotrienol	γ-Tocotrienol	δ-Tocotrienol	Total (mg/kg)
n-hexane	32.4 – 34.5	3.4 – 3.8	56.4 – 56.7	4.0 – 4.4	1,372
SC-CO_2	37.1 – 38.3	2.1 – 2.4	54.2 – 55.8	4.2 – 4.5	1,263

Table 4. Sterols content of *E. oleifera* mesocarp oil.

Extraction method	Sterols composition of *E. oleifera* mesocarp oil (%)				
	Cholesterol	Campesterol	Stigmasterol	β-Sitosterol	Total (mg/kg)
n-hexane	ND	18.8 – 20.1	11.3 – 13.4	65.7 – 67.2	1,203
SC-CO_2	ND	18.5 – 19.7	12.2 – 13.1	66.3 – 68.4	1,173

Note: ND – not detected

squalene in *E. oleifera* was 3 to 4 times that of the *E. guineensis* palm oil.

Fractionation of oils and fats or their ester derivatives to obtain valuable products with better functionality such as ώ-3 fatty acids, tocopherols, squalene, carotenes and sterols using SC-CO_2 has been demonstrated earlier [7,14,15,16,17]. The solubility differences between vitamin E, sterols, squalene and carotenes at specific extraction conditions will enable the separation and isolation of these compounds from *E. oleifera* into enriched fractions.

FA composition of *E. oleifera* kernel oil

The yield of kernel oil was 19.2% based on the dried kernels. The kernel oil from *E. oleifera* was extracted using *n*-hexane and the FAC was analyzed and compared to the *E. guineensis* palm oil (Table 5). There was 27% of 18:1 fatty acid in *E. oleifera* kernel oil compared to 15% in normal *Tenera* kernel oil. However, lower 12:0 fatty acid content was detected in *E. oleifera* at 29% compared to 48% in typical *Tenera* kernel oil.

SC-CO_2 extraction of *E. oleifera* palm oil has been proven to be technically viable. By manipulating the extraction conditions, it is believed that fractions of oil enriched with desired minor components can be produced and formulated into dietary supplements.

Acknowledgements – The authors would like to thank the Director General of MPOB for his permission to publish this paper.

Table 5. Fatty acids compositions of extracted kernel oils.

Carbon chain length	Percentage (%)		
	Hexane extracted *E. oleifera* kernel oil	SC-CO_2 extracted *E. oleifera* kernel oil	*E. guineensis* kernel oil[a]
1. 8:0	1.3 – 1.5	1.4 – 1.5	4.4
2. 10:0	1.3 – 1.4	1.2 – 1.3	3.7
3. 12:0	27.6 – 28.9	28.5 – 2 9.4	48.3
4. 14:0	21.4 – 22.6	20.3 – 22.1	15.6
5. 16:0	8.7 – 9.9	9.6 – 10.4	7.8
6. 16:1	0.1 – 0.2	0.1 – 0.2	0.1
7. 18:0	3.1 – 3.3	3.0 - 3.4	2.0
8. 18:1	27.1 – 28.0	26.8 – 27.6	15.1
9. 18:2	4.9 – 5.5	5.1 – 5.6	2.7
10. 20:0	0.1 – 0.2	0.1 – 0.2	0.2

[a] Data obtained from *Pocketbook of Palm Oil Uses* [18].

REFERENCES

1. Choo Y.M. and Yusof B. (1996) Elaeis Oleifera Palm for the Pharmaceutical Industry. *PORIM Information Series,* TT No. **42.**
2. List G.R., Friedrich J.P. and Pominski J. (1984) Characterization and Processing of Cottonseed Oil Obtained by Extraction with Supercritical Carbon Dioxide. *J. Am. Oil Chem. Soc.* **61:** 847-1849.
3. List G.R., King J.W., Johnson J. H., Warner K. and Mounts T.L. (1993) Supercritical Degumming and Physical Refining of Soybean Oil. *J. Am. Oil Chem. Soc.* **70:** 473-476.
4. Mendes M.F., Pessoa F.L.P. and Uller A.M.C. (2002) An Economic Evaluation Based on an Experimental Study of the Vitamin E Concentration Present in Deodorizer Distillate of Soybean Oil using Supercritical CO_2. *J. Supercritical Fluids* **23:** 257-265.
5. List G.R., Friedrich J.P. and Christianson D.D. (1984) Properties and Processing of Corn Oils Obtained by Extraction with Supercritical Carbon Dioxide. *J. Am. Oil Chem. Soc.* **61:** 1849-1851.
6. Montanari L., Fantozzi P., Snyder J.M. and King J.W. (1999) Selective extraction of phospholipids from soybeans with supercritical carbon dioxide and ethanol. *J. Supercritical Fluids* **14:** 87.
7. Choo Y.M., Ma A.N., Hawari Y., Yamauchi Y., Bounoshita M. and Saito M. (1996) Separation of Crude Palm Oil Components by Semi-Preparative

Supercritical Fluid Chromatography. *J. Am. Oil Chem. Soc.* **73:** 523-525.

8. Choo Y.M., Yap S.C., Ooi C.K., Ma A.N., Goh S.H. and Ong A.S.H. (1996) Recovered Oil from Palm-Pressed Fiber: A Good Source of Natural Carotenoids, Vitamin E and Sterols. *J. Am. Oil Chem. Soc.* **73:** 599-602.
9. Markom M., Singh H. and Hasan M. (2001) Supercritical CO2 Fractionation of Crude Palm Oil, *J. Supercritical Fluids.* **20:** 45-53.
10. Malaysian Palm Oil Board. (2005) MPOB Test Methods: Determination of Carotene Content. **p2.6:** 194-197, *Malaysian Palm Oil Board,* Selangor, Malaysia.
11. Lau H.L.N., Puah C.W., Choo Y.M., Ma A.N. and Chuah C.H. (2005) Simultaneous Quantification of Free Fatty Acids, Free Sterols, Squalene and Acylglycerol Molecular Species in Palm Oil by using High-Temperature GC-FID. *Lipids* **40:** 523-528.
12. Choo Y.M., Ma A.N. and Yap S.C. (1997) Carotenes, Vitamin E and Sterols in Oils from Elaeis guineensis, Elaeis oleifera and Their Hydrids. *Palm Oil Developments* **27:** 1-9.
13. List G.R., King J.W., Johnson J.H., Warner K. and Mounts T.L. (1993) Supercritical Degumming and Physical Refining of Soybean Oil. *J. Am. Oil Chem. Soc.* **70:** 473-476.
14. Ibanez E., Benavides A.M.H., Senorans F.J. and Reglero G. (2002) Concentration of Sterols and Tocoplerols from Olive Oil with Supercritical Carbon Dioxide. *J. Am. Oil Chem. Soc.* **79:** 1255-1260.
15. Nilsson W.B., Gauglitz E.J., Hudson J.K., Sout V.F. and Spinelli J. (1989) Fractionation of Fish Oil Esters Using Incremental Pressure Programming and Temperature Gradient. *J. Am. Oil Chem. Soc.* **66:** 1596-1600.
16. Ghosh S. and Bhattacharyya D.K. (1996) Isolation of Tocopherol and Sterol Concentrate from Sunflower Oil Deodorizer Distillate. *J. Am. Oil Chem. Soc.* **73:** 1271-1274.
17. Lee H., Chung B.H. and Park Y.H. (1991) Concentration of Tocopherols from Soybean Sludge by Supercritical Carbon Dioxide. *J. Am. Oil Chem. Soc.* **68:** 571-573.
18. Pantzaris T.P. (2000) *Pocketbook of Palm Oil Uses* (5th ed.) Malaysian Palm Oil Board, Selangor, Malaysia.

Journal of Science and Technology in the Tropics (2007) **3:** 39-43

2-Fluoropyrimidine: A potential fluorogenic reagent

Z. Abdullah, M. A. A Bakar, Z. Aiyub and R. Yahya
Department of Chemistry, Faculty of Science, University of Malaya
50603 Kuala Lumpur, Malaysia
(Email: zana@um.edu.my)

Received 24.03.2006; accepted 01.02.2007

Abstract Derivatives of non-fluorescent 2-fluoropyrimidine such as 2-*N*-methylaminopyrimidine, 2-*N*-ethylaminopyrimidine, 2-*N*-piperidinopyrimidine, 2-*N*-anilinopyrimidine and 2-*N*-methylanilinopyrimidine were examined for their fluorescence properties. 2-N-methylaminopyrimidine fluoresced at 377 nm, when excited at 282 nm, 2-*N*-ethylaminopyrimidine fluoresced at 375 nm with excitation wavelength of 286 nm, 2-*N*-piperidinopyrimidine fluoresced at 404 nm when excited at 286 nm. Derivatives of aromatic amines such as 2-*N*-anilinopyrimidine showed fluorescence peak at 434 nm, when excited at 358 nm and 2-*N*-methylanilinopyrimidine fluoresced at 406, when excited at 288 nm. Fluorescence peaks were also observed with 2-phenoxy and other phenol derivatives. No fluorescence peak was observed with amino acid derivatives.

Keywords fluorescence – alkylaminopyrimidines – phenoxypyrimidine

INTRODUCTION

The advancement in the field of biology and chemistry today is limited by the availability of sensitive analytical techniques. These analytical techniques are very important especially in studies that involve low concentrations [1, 2] and for detection of organic compounds in various media. In organic and analytical chemistry, the detection of aliphatic and/or aromatic pollutants is very important especially in water. The detection of these pollutants can be carried out fluorimetrically or using combination of techniques, as in the detection of phenols. Recently, the use of fluorescence spectrometer has been widely used in detecting organic pollutants.

In general, fluorescence spectrometer has been used to analyse amines in the early 1960s. Most aliphatic amines are non-fluorescent whereas the majority of aromatic amines and phenols are fluorescent compounds. Amines which possess fluorescent characteristic can be detected fluorimetrically without the need of chemical modification [3, 4]. For example, serotonin i.e. 5-hydroxy tryptamine, is highly fluorescent in aqueous solution [5], hence its detection can be conducted without any chemical modification. For non-fluorescent amines, chemical and structure modification is needed before it can be detected fluorimetrically. For example, the estimation of histidine and histamine in peptide extracts is normally carried out by condensing with *o*-pthaldehyde. The product formed with histidine is less fluorescent compared to histamine derivative. Thus, in estimating histidine, it is first converted to histamine followed by condensing with *o*-pthaldehyde [6] and detected fluorimetrically.

This work involves synthesising various fluorogenic reagents, that can be used to detect and speciate amines, phenol and/or amino acids based on their fluorescence characteristics. In this paper, the potential of 2-fluoropyrimidine as the fluorogenic reagent and the fluorescence characteristic of alkylamino, arylamino and phenoxy derivatives will be discussed.

Journal of Science and Technology in the Tropics (2007) 3: 39-43

MATERIALS AND METHODS

General

^{1}H-NMR and ^{13}C-NMR spectra were recorded using a JOEL JNM-GSX 270 NMR Instrument. Mass spectra were recorded using a GCMS Hewlett-Packard HP 6890 with a mass selective indicator, and infra red spectra were recorded using a Perkin Elmer 298 Infra red spectrometer.

Alkylaminopyrimidines syntheses

2-*N*-Methylaminopyrimidine, 2-*N*-ethylaminopyrimidine, 2-*N*-piperidinopyrimidine and 2-phenoxypyrimidine were obtained as described in our previous studies [9-10]. 2-*N*-Anilinopyrimidine was prepared according to Chapman and Hall's method [11].

Preparation of 2-*N*-methylanilinopyrimidine

2-Fluoropyrimidine (0.20 g, 2.041 mmol) was added to *N*-methylaniline (0.2 mL, 2.198 mmol) and the mixture was heated in an oil bath at 140° C for 3 hours. The heating was stopped when the starting material could no longer be detected on a thin layer chromatography. The product was obtained from sublimation process which was carried out at 185-190°C under reduced pressure. The product was recrystallised from ethyl-acetate:chloroform (2:1) to give a pure green transparent plate-like crystals (0.150 g). Yield: 46%, 179-182°C,: ^{1}H-NMR (δ): 6.93 (t, 1H, H-5 of pyrimidine ring), 7.27-7.58 (m, 5H, H-2, H-3, H-4, H-5 and H-6 of benzene ring), 8.64 (d, 2H, H-4 and H-6 of pyrimidine ring), 3.84 (s, 3H, H -C***H***$_3$); ^{13}C-NMR (δ): 141.45 (C-1 of benzene ring), 109.85 (C-5 of pyrimidine ring), 130.48 (C-4 and C-6 of pyrimidine ring), 154.18 (C-2 of pyrimidine ring), 126.29 (C-3, C-4 and C-5 of benzene ring), 129.04 (C-2 and C-6 of benzene ring), 41.20 (CH_3): MS: M^+ = 185.2, $C_{11}H_{11}N_3$ requires M^+ = 185.093.

Preparation of 2-(2-methyl)phenoxypyrimidine

Sodium metal (1.1 g) was added to *o*-cresol (5 mL, 48.5mmol). The mixture was stirred for 10 minutes at room temperature. 2-Fluoropyrimidine (0.15 g, 1.5306 mmol) was then added to reaction mixture. The reaction mixture was refluxed under constant stirring for two hour, and then cooled. Water (10 mL) was then added to the mixture and extracted with ether (2 x 15 mL). The ethereal extracts were washed with water and dried over anhydrous sodium sulphate. Evaporation of solvent gave crude product which was recrystallised from hexane:acetone (4:1) to give yellow plate-like crystals (0.118 g): Yield: 46%, 75-77°C,: IR (cm^{-1}): 1112.6; ^{1}H-NMR (δ): 7.13 (t, 1H, H-5 of pyrimidine ring), 7.21-7.41 (m, 4-H, H-3, H-4, H-5, H-6 of benzene ring), 8.66 (d, 2H, H-4 and H-6 of pyrimidine ring), 2.30 (s, 3H, C***H***$_3$); ^{13}C-NMR (δ):115.86 (C-5 of pyrimidine ring), 159.77 (C-4 and C-6 of pyrimidine ring), 165.15 (C-2 of pyrimidine ring), 151.25 (C-1 of benzene ring), 121.85 (C-4 of benzene ring,) 125.80 (C-3 of benzene ring), 128.09 (C-5 of benzene ring), 131.32 (C-6 of benzene ring,), 130.57 (C-2 of benzene ring), 16.25 (CH_3): MS: M^+ = 186.2, C11H11N2O requires M^+ = 186.079.

Preparation of 2-(3-methyl)phenoxypyrimidine

Sodium metal (1.0 g) was added to *m*-cresol (5 mL, 47.8 mmole). The mixture was stirred for 10 minutes at room temperature. 2-Fluoropyrimidine (0.16 g, 1.633 mmole) was then added to *m*-cresol. The reaction mixture was refluxed under constant stirring for one hour. The mixture was cooled, water (10 mL) was added to the mixture. The mixture was then extracted with ether (4 x 10 mL). The combined ethereal layer was washed with water and dried over anhydrous sodium sulphate. Evaporation of solvent gave crude product which was recrystallised from hexane:chloroform to give 0.101g of yellow crystals: Yield: 38.8%, 78-80°C,: ^{1}H-NMR (δ): 7.31 (t, 1H, H-5 of pyrimidine ring), 7.00-7.08 (m, 4H, H-2, H-4, H-5 AND H-6 of benzene ring), 8.55 (d, 2H, H-4 and H-6 of pyrimidine ring), 2.38 (s, 3H, C***H***$_3$); ^{13}C-NMR (δ):129.36 (C-5 of pyrimidine ring), 159.71 (C-4 and C-6 of pyrimidine ring), 165.52 (C-2 of pyrimidine ring), 152.71 (C-1 of benzene ring), 122.21 (C-4 of benzene ring) 139.85 (C-3 of benzene ring), 126.39 (C-5 of benzene ring), 116.05 (C-6 of benzene ring), 118.62 (C-2 of benzene ring, 21.40 (CH_3): MS: M^+ = 186.2, C11H11N2O requires M^+ = 186.079.

Preparation of 2-glycinopyrimidine

2-Fluoropyrimidine (0.3 g, 0.316 mmol) was dissolved in 75% ethanol (10 mL) and added to an alkaline solution of glycine (0.4 g, 5.33 mmol, in 4 mL 0.1M sodium hydroxide). The mixture

was refluxed for 10 minutes, followed by another addition of 0.1M sodium hydroxide (4 mL). The mixture was refluxed for another 45 minutes. The mixture was cooled and ethanol was evaporated off. A minimum volume of water was added to the residue and the pH of the solution was adjusted to pH 7. The mixture was then shaken in ether. The ethereal layer was discarded. The pH of the aqueous was further adjusted to pH 4.3 and extracted three times with ether (3 x 10 ml). The ethereal layer was then washed with water and dried. Evaporation of ether gave crude product; pure 2-glycinopyrimidine was obtained after separating from traces of starting material using column chromatography. Yield: 15%, darkens above 165-167°C; IR (cm^{-1}): 3275, 1678, 1665, 1618; ^{1}H-NMR (δ): 8.22 (d, 2H, H-4 and H-6 pyrimidine ring), 7.15 (b, 1H, N**H**), 6.56 (t, 1H, H-5 of pyrimidine ring), 3.96 (s, 2H, H of -N-C$\boldsymbol{H}_2$COOH) MS: M^+= 153.0; $C_6H_7N_3O_2$ requires M^+=153.054.

Preparation of 2-phenylalaninopyrimidine

2-Fluoropyrimidine (0.27 g, 2.733 mmol) was dissolved in 75% ethanol (8 mL) and added to a solution of phenylalanine (0.445 g, 2.697 mmol) in 0.1M sodium hydroxide (10 mL). The mixture was refluxed for 5 minutes, followed by another addition of 0.1M sodium hydroxide (10 mL). The mixture was refluxed for another 30 minutes. The mixture was cooled and ethanol was evaporated off. A minimum volume of water was added to the residue and the pH of the solution was adjusted to pH 7. The mixture was then shaken in ether and the ethereal layer was discarded. The pH of the solution was further adjusted to pH 3.3 and extracted three times with ether (3 x 7 ml). The ethereal layer was washed with water (2 x 10 mL) and dried. Ether was distilled off. Pure 2-phenylalaninopyrimidine was obtained using preparative thin layer chromatography. Yield: 25%, darkens above 150°C; IR (cm^{-1}): 3115, 1675, 1660, 1600; ^{1}H-NMR (δ): 8.18 (d, 2H, H-4 and H-6 pyrimidine ring), 7.20 (m, 5H, H-2, H-3 H-4, H-5 and H6 (-NHCH($CH_2C_6\boldsymbol{H}_5$)COOH) of benzene ring), 7.05 (b, 1H, N$\boldsymbol{H}$), 6.53 (t, 1H, H-5 of pyrimidine ring), 4.47 (m, 1H, H of -NHC$\boldsymbol{H}$($CH_2C_6H_5$) COOH), 3.07 (m, 2H, -NHCH(C$\boldsymbol{H}_2$C6H5)COOH)); MS: M^+= 242.1; $C_{13}H_{13}N_3O_2$ requires M^+=243.101.

General procedure for fluorescence measurements

Ethanolic solutions (10mL) of alkylaminopyrimidines and phenoxypyrimidines (1.168 x 10^{-3} M) were prepared. The fluorescence measurement was recorded using a quartz cell at room temperature using a Hitachi Model 200 Fluorescence Spectrometer. The sensitivity of the instrument was 2.00. Phenol was used as the standard and the fluorescence intensity of phenol was taken to be 1.00.

RESULTS AND DISCUSSION

The structures of 2-*N*-alkylaminopyrimidines, 2-*N*-anilinopyrimidines, 2-phenoxypyrimidines and derivatives of amino acids studied are as shown in Figure 1.

Structure	Name	Structure	Name
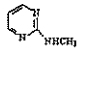	2-*N*-methylamino		2-phenoxy
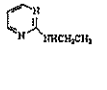	2-*N*-ethylamino		2-(2-methyl)phenoxy
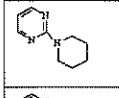	2-*N*-piperidino	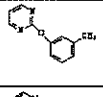	2-(3-methyl)phenoxy
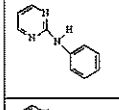	2-*N*-anilino	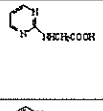	2-glycino
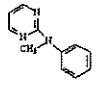	2-*N*-methylanilino	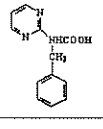	2-phenylalanino

Figure 1. The structure of the derivatives of pyrimidines.

Fluorescence studies show that 2-fluoropyrimidine, methylamine, ethylamine and piperidine are non fluorescent compounds, whereas aniline and *N*-methylaniline showed fluorescence band at 325 nm and 337 nm respectively when excited at 276 nm and 278 nm as shown in Table 1.

Table 2 shows the fluorescence characteristic of 2-alkylamino and 2-arylaminopyrimidine in ethanol. It can be seen from the table that 2-*N*-methylaminopyrimidine fluoresced at 377 nm when excited at 282 nm, 2-*N*-ethylaminopyrimidine showed fluorescence peak at 375 nm when excited at 286 nm, 2-*N*-piperidinopyrimidine fluoresced at 404 nm when excited at 286 nm, 2-*N*-anilinopyrimidine showed fluorescence peak at 434 nm when excited at 358 nm and 2-*N*-methylanilinopyrimidine fluoresced at 406 nm when excited at 288 nm.

It can also be seen from the table 2 that 2-*N*-anilinopyrimidine showed the highest relative fluorescence intensity and 2-*N*-piperidinopyrimidine showed the least. 2-Arylaminopyrimidines fluoresced at a longer wavelength compared to 2-alkyaminopyrimidines.

The fluorescence peaks of arylaminopyrimidines which are recorded at longer wavelengths are due to an increase in conjugation in the system. The increase in conjugation results in the free mobility of π electrons in the system, thus shifting the fluorescence wavelength to higher value. The increase in conjugation in the systems also allows π electrons to be more delocalized within the system and as the results an increase in the relative fluorescence intensity was observed.

2-*N*-Piperidinopyrimidine has the least relative fluorescence intensity amongst 2-alkylamino derivatives. The lower fluorescence intensity observed is believed to be due to the piperidino ring flipping from one conformation to another losing energy during the process [9].

The low fluorescence intensity of 2-*N*-methylanilinopyrimidine compared with 2-*N*-anilinopyrimidine is probably due to the non-rigidity of 2-*N*-methylanilinopyrimidine. The presence of a methyl group in 2-*N*-methylanilinopyrimidine makes the compound less rigid and the energy is lost through either vibration or rotation of the

Table 1. Fluorescence characteristic of starting materials in dichloromethane.

Compound	Excitation wavelength/nm	Fluorescence peak/nm	Relative fluorescence intensity
Aniline	276	325	0.0341
N-Methylaniline	281	337	0.0161
2-Fluoropyrimidine	Non- fluorescent		
Methylamine	Non- fluorescent		
Ethylamine	Non- fluorescent		
Piperidine	Non- fluorescent		

Table 2. Fluorescence peak of alkylamino and arylaminopyrimidines in ethanol.

2-X pyrimidine	Excitation wavelength/nm	Fluorescence peak/nm	Relative fluorescence intensity
2-*N*-methylamino	282	377	0.0427
2-*N*-ethylamino	286	375	0.0440
2-*N*-piperidino	286	404	0.0351
2-*N*-anilino	358	434	0.2996
2-*N*-methylanilino	288	406	0.1752

Table 3. Fluorescence peaks of phenoxy and amino acid derivatives in ethanol.

2-X pyrimidine	Excitation wavelength/nm	Fluorescence peak/nm	Relative fluorescence intensity
2-phenoxy	285	308	0.1301
2-(2-methyl)phenoxy	283	305	0.1032
2-(3-methyl)phenoxy	285	310	0.1025
2-phenylalanino	Non-fluorescent		
2-glycino	Non-fluorescent		

methyl group.

The fluorescence peaks of phenol and amino acid derivatives are as shown in Table 3. 2-Phenoxypyrimidine is the most fluorescent amongst the phenoxy derivatives, whereas amino acid derivatives are non-fluorescent. The decrease fluorescence intensity observed with 2-(2-methyl)phenoxypyrimidine and 2-(3-methyl)phenoxypyrimidine is believed to be due to the same reason as in the case of 2-*N*-methylalaninopyrimidine discussed earlier. No fluorescence peak was observed with amino acid derivatives, which is probably due to the presence of a carboxyl group, an electron withdrawing substituent. Apart from the presence of an electron withdrawing substituent which tends to reduce the fluorescence intensity, the acid amino derivatives are believed to be in *N*-protonated form. Earlier study [12, 13] has shown that the undissociated carboxyl group interacts with the excited aromatic ring and pyrimidine ring [13] causing quenching to occur. This quenching effect results from the intermolecular charge transfer and thus explain the non-fluorescent or low fluorescent intensity observed with all amino acid derivatives.

CONCLUSION

2-*N*-Alkylaminopyrimidines, 2-*N*-arylaminopyrimidines, 2-phenoxypyrimidines, 2-glycino and 2-phenylalaninopyrimidines were obtained by reacting 2-fluoropyrimidine with respective amines, phenols and amino acids. Preliminary studies show that 2-alkylaminopyrimidines, 2-arylaminopyrimidines and 2-phenoxypyrimidines are fluorescent compounds, whereas 2-glycino and 2-phenylalaninopyrimidines are non-fluorescent.

REFERENCES

1. McCaman M.W. and Robins E. (1952) *J. Clin. Med.* **59:** 885.
2. Wong K. (1972) *Anal Biochem.* **49(1):** 73.
3. Kreps S.F., Druin M. and Czorny B. (1965) *Anal. Chem.* 1965: 37, 586
4. Sopes R.K. (1972) *Anal. Biochem.* **49 (1):** 73.
5. Udenfriend U., Weissabatch H. and Clark C.T. (1963) *J. Biochem.* **37:** 586.
6. Shere P.A., Burkhartter M. and Cohn V.H. Jr. (1959) *J. Pharmacol. Expt. Therap.* **27:** 82.
7. Brown D.J. and Waring P. (1974) *J. Chem Soc. Perkin Trans.* 204.
8. Abdullah Z., Mohd Tahir N., Abas M.R. and Low B.K (1996) *Jour. Science* **4(1):** 417.
9. Abdullah Z., Mohd Tahir, N., Abas M.R., Aiyub Z. and Low B.K. (2004) *Molecules* **9:** 520.
10. Abdullah Z. (2005) *Int. J. Chem. Sci.* **3**(1): 9-15.
11. Brown D.J. and Waring P. (1974) *J. Chem. Soc, Perkin Trans II:* 204.
12. Feitelson J. (1964) *J. Phys Chem.* **68:** 391.
13. Abdullah Z., A. Bakar M.A., Mohd Shariffuddin M.A and Aiyub Z. (2006) *Malaysian Jour. Chemistry* – accepted.

Journal of Science and Technology in the Tropics (2007) **3:** 45-50

Changes in physicochemical characteristics of oil palm frond after NaOH treatment towards improved heavy metal sorption

A. Z. Abdullah*, B. Salamatinia, N. Razali and A. H. Kamaruddin
School of Chemical Engineering, Universiti Sains Malaysia, Engineering Campus,
14300 Nibong Tebal, Penang, Malaysia
(*Email: chzuhairi@eng.usm.my)

Received 12.10.2006; accepted 25.01.2007

Abstract NaOH treatment on oil palm frond (OPF) was investigated for improvement in copper (Cu) and zinc (Zn) sorption from aqueous solution. The OPF was chemically modified by soaking it in 0.6 M NaOH solution for 45 min, followed by washing and drying. The sorption process of Cu and Zn was carried out in an orbital shaker and shaken at 150 rpm using metal solutions at 100 ppm. Increased heavy metal sorption capacity of the OPF resulted after NaOH treatment. Changes in surface morphology and elemental composition analysis suggested the solubilization of hemicellulose or pectin from OPF, detected by material shrinkage and reduced –CH3 amount. Na was the counter ion in the treated biomass for exchange with heavy metals as suggested by thermogravimetry analysis (TGA). The higher nitrogen-containing groups in NaOH-treated OPF as detected through elemental analysis acted as the positively charged functional groups that bound Na to be subsequently exchanged with heavy metal during the sorption process. Other functional groups that could play the same role, but of less importance, were the sulphur-containing groups.

Keywords Oil palm frond – NaOH – heavy metal – sorption – physicochemical characteristics

INTRODUCTION

Heavy metals are among the most common pollutants found in industrial wastewater and conventional methods for heavy metal removal are often ineffective, uneconomical or technically complicated [1]. Current research on heavy metal removal is moving towards the use of low-cost sorbent materials [2, 3]. Being a tropical country, Malaysia has an enormous supply of biomass resources generated mainly from agricultural activities. Currently, Malaysia is the leading producer of palm oil in the world and this industry also generates about 50 million tonnes of biomasses in 2005 [4]. These biomasses are mainly in the form of palm press fibre (PPF), empty fruit bunch (EFB), shell and oil palm frond (OPF). Therefore, the utilization of those biomasses for value-added applications such as in the sorption of heavy metals needs to be explored and investigated.

Interest has risen in removing heavy metals by sorption on agricultural materials such as waste wool, nut wastes, tree barks, modified cotton and sawdust [5]. These agricultural wastes, which are biopolymers in nature, possess a variety of functional groups such as hydroxyl groups to which other moieties can be reacted for possible enhancement in the efficiency of metal ion sorption [1, 6]. The sorption properties of the biomass can be improved or modified by several methods [5-7].

NaOH pretreatment has been reported in the literature to potentially improve the heavy metal sorption of various biomasses [8]. However, there is little report on the use of NaOH treated OPF for this application. The chemical composition of this oil palm biomass could be significantly different from those reported and treatment with NaOH could result in heavy metal binding sites that are significantly different in chemical natures [7]. Since the heavy metal sorption onto the biomass is mainly governed by the number and types of active binding sites present on the surface, it is of great interest

to elucidate the behaviour and performance of NaOH treated OPF in this particular environmental application. In this study, oil palm frond has been investigated for sorption of copper (Cu) and zinc (Zn) ions from aqueous solution. Our earlier study showed that NaOH treatment of OPF could improve its heavy metal uptake and the treatment conditions have been optimized [9]. Particular focus was given to the elucidation and characterization of the physicochemical changes that occurred after treatment of OPF with NaOH solution and consequently led to the improvement in its heavy metal sorption capacity.

MATERIALS AND METHODS

Sorbent preparation and modification

OPF sample obtained from oil palm tree in Nibong Tebal, Penang, Malaysia was first cut into small pieces, ground with a blender (Epicson Eb-321) for 1 min, washed thoroughly with water and dried in an oven at 70°C for 12 h. For the modification of OPF, 0.6 M NaOH was used to soak 2.5 g of OPF at room temperature for 45 min in a conical flask. The treated biomass was washed thoroughly with distilled water and dried in an oven at 70°C for 12 h.

Heavy metal sorption

The heavy metal sorption was carried out using 250 mL of Cu or Zn solution at 100 ppm with 1 g of OPF sorbent at room temperature. The flask was shaken in an orbital shaker at 150 rpm for the desired contact time. The solid-liquid mixture was then filtered and the residual heavy metal concentration in the filtrate was measured either using a copper meter (Hanna HI 93702) or a zinc meter (Hanna HI 93731). These meters provided a rapid and accurate way to measure the heavy metal concentration in aqueous solutions. They also show high degree of reproducibility (within 1 %) in the data obtained. The results obtained using these meters were and no significantly different (at 99 % confidence level) from those obtained using AAS.

Characterization

All OPF sorbents were characterized using Fourier-transformed infra red (FTIR) spectrophotometer (Perkin Elmer 2000), scanning electron microscopy (SEM) (Leo supra 50 VP), thermogravimetry analyzer (Perkin Elmer TGA7) and elemental analyzer (Perkin Elmer Series II 2400).

RESULTS AND DISCUSSION

Heavy metal sorption process

The untreated OPF showed low capability for heavy metal sorption (Fig. 1). After 120 min of contact time, this sorbent was only able to remove less than 10 % of the heavy metals. The removal efficiency showed an increase in the first 60 min and then almost constant at longer contact times. Similar removal trend was demonstrated by both heavy metals. This trend suggested low number of active metal binding sites in the untreated OPF. Initially, these sites were available for sorption of heavy metal ions leading to a steady increase in the metal removal. Upon saturation, the sorption process was governed by the net rate of the sorption and desoprtion processes [10].

NaOH treatment of OPF brought about a dramatic improvement in the removal efficiency of the sorbent. For example, removal efficiencies of 49 % and 40 % for Cu and Zn, respectively were achieved within 5 min, compared to 2 % and 3 % with the untreated OPF. Almost complete sorption was observed at about 30 min for both metals, after which, no significant increase was detected. The corresponding maximum metal uptake capacities (measured after 90 h of contact time i.e. when equilibrium concentration had been reached) achieved with this NaOH treated OPF were 14.8 mg/g and 13.6 mg/g for Cu and Zn, respectively. Sorption of Cu ions on the treated and untreated OPF sorbents was higher than Zn ions (Fig. 1).

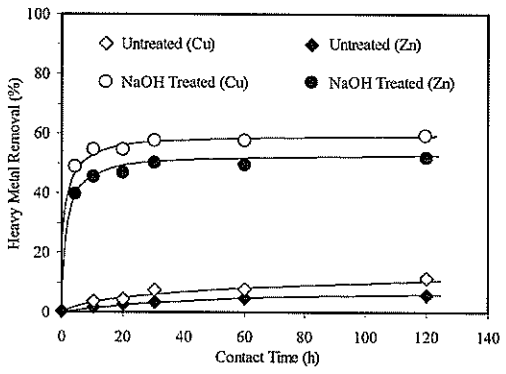

Figure 1. Copper (Cu) and zinc (Zn) removals by the untreated and NaOH treated OPF.

This could be associated with the ionic size of those metals that in turn affected the strength of the interaction with the binding sites in the OPF sorbent [11].

Drastic increase in the sorption efficiency of OPF upon treatment with NaOH was deemed to be caused by the introduction of active metal binding sites of different chemical natures in the sorbent material. This was based on the observation that the magnitude of improvement was so high (6-10 times) while the time taken to reach equilibrium was reduced to almost one-fourth with NaOH treated OPF. Similar conclusion was obtained with the sorption of cadmium ions on NaOH treated cyanobacterium *Tolypothrix tenuis* [12]. The structural changes originating from the solubilization of hemicellulose and pectin, the two primary components of OPF, upon treatment with NaOH were deemed to be the main changes. This is similar to the findings of sugar beet pulp for the same role [13].

In this study, the commonly used isotherms to represent the sorption process such as the Langmuir and Freundlich isotherms did not fit accurately with the experimental data, with R2 values of 0.82 and 0.88, respectively. This observation suggests that some of the main assumptions made by the isotherm models are not valid for this particular sorption system.

Biomass characterization

Fourier transform infrared (FTIR) spectrophotometry

IR spectra of the raw and chemically modified OPF biomass were obtained to investigate the effects of chemical treatment on the functional groups of the biomass which might be involved in the sorption of heavy metals (Fig. 2). For the raw OPF biomass the trough observed at 3,437 cm^{-1} results from the NH_2 aromatic amines or primary amines while that observed at 2,919 cm^{-1} is indicative of C–H strech in C–CH_3 terminal groups which confirmed the presence of pectin in the biomass [12]. At a wavenumber of 1,637 cm^{-1}, the trough observed might be the result of tertiary amides conjugated to a mono or distributed C=C [14]. The same trough has been found in the FTIR spectra of *Aspergillus niger* [7]. The trough at 1,384 cm^{-1} indicates –SO_2H antisym stretch mode while that of carboxylic group is observed at 1,319 cm^{-1}. The presence of primary

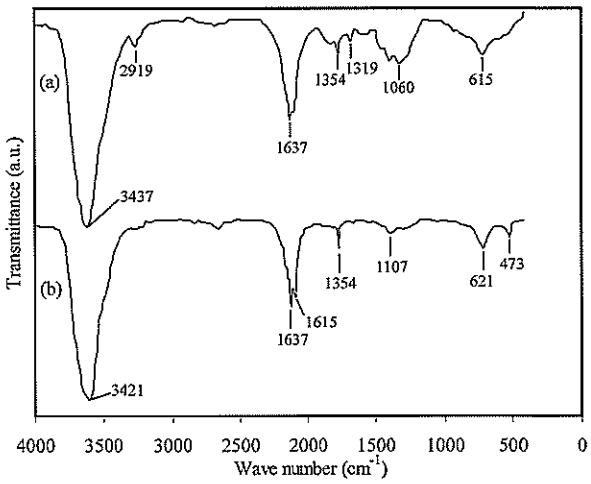

Figure 2. Fourier-transformed infra red spectrum of OPF. (a) before NaOH treatment, and (b) after NaOH treatment.

aliphatic amines group (-C-NH_2) is indicated by the presence of a weak band in the range of 1,030 - 1,120 cm^{-1} [6].

For OPF after the treatment with NaOH the spectra shows the same characteristic troughs as in the untreated biomass, i.e. at 3,421 cm^{-1}, 1,637 cm^{-1}, 1,384 cm^{-1}, 1,107cm^{-1} and 621cm^{-1}. The absence of troughs at 2,919 cm^{-1} and 1,319 cm^{-1} indicated the removal of terminal –CH_3 and carboxyl groups in the biomass. This is attributed to the dissolution of pectin and hemicellulose into the NaOH solution during the NaOH treatment process.

The FTIR results suggested that the metal binding group could be partly in the form of the NH_2 aromatic amines observed as a through at 3,437 cm^{-1} or tertiary amides as detected at 1,646 cm^{-1}. The presence of primary aliphatic amines as group (-C-NH_2), indicated by the presence of bands in the range of 1,030–1,120 cm^{-1}, could also be the effective functional group in the metal sorption process.

Scanning Electron Microscopy (SEM)

SEM micrographs of OPF obtained before and after NaOH treatment (Fig. 3) indicated that the NaOH treatment made the surface area of the biomass softer and reduced the porosity. In other words, the base treatment led to biomass shrinkage. This was mainly due to the solubilisation of hemicellulose and pectin after NaOH treatment [13].

In contrast to cellulose that is crystalline, strong

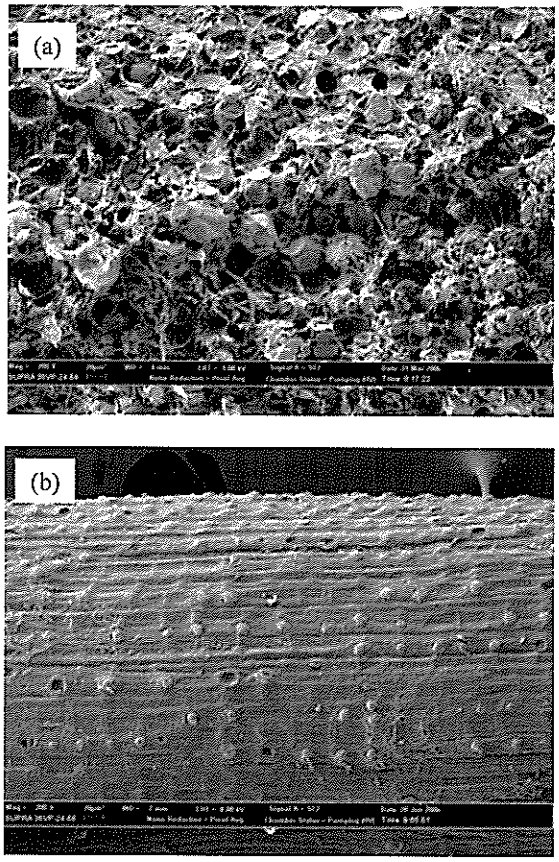

Figure 3. SEM image of OPF. (a) before NaOH treatment, and (b) after NaOH treatment.

and resistant to hydrolysis, hemicellulose has a random, amorphous structure with little strength and could be easily hydrolyzed by dilute acid or base [11]. As hemicellulose served to bind pectin to cellulose to form a network of cross-linked fibres in OPF [15], the shrinkage of the biomass upon the extraction of these two primary structural components was to be expected. The pectin and hemicellulose removal was also confirmed by the results obtained from the FTIR which indicated the disappearance of $-CH_3$ bands from the biomass. Generally, pectins form most of the molecules, in blocks of hairy regions [10]. The SEM images showed that after the treatment the hairy surface of the biomass disappeared.

Elemental composition

The elemental analyzer was used in order to measure the weight composition of carbon (C), hydrogen (H), nitrogen (N) and sulphur (S) in the OPF sorbents. The carbon content was slightly reduced in NaOH treated OPF while hydrogen content showed a slight increase (Table 1). However, the C/H ratio was found to decrease, suggesting the removal of higher C/H ratio fractions. In both sorbents, a small amount of sulphur (<1.0 %) was also detected. The sulphur content detected could be in the form of negatively charged sulphur-containing groups, which could play the role as the binding site for accepting the Na^+ ions after NaOH treatment to be subsequently exchanged with the heavy metal ions during the sorption process. The nitrogen content showed a significant increase in the treated OPF.

Table 1. Carbon, hydrogen and sulphur composition in treated and untreated OPF as determined by elemental analyzer.

Material	Composition (wt %)			
	Carbon	Hydrogen	Nitrogen	Sulphur
Untreated	43.2	9.1	1.4	0.9
NaOH treated	41.1	9.2	4.7	0.9

Treatment of OPF with NaOH increased the nitrogen content of the biomass to 4.7 %. This was contributed by the removal of some hydrocarbon constituent of the biomass during NaOH treatment while the nitrogen-containing fraction remained. In this respect, the pectin and hemicellulose fractions of the OPF do not contain nitrogen-containing functional groups [5]. This result was in agreement with the results obtained from FTIR analysis that indicated the presence of amine groups after the NaOH treatment. Slightly higher nitrogen content as detected in the NaOH treated OPF biomass suggested the nitrogen-containing functional groups to be the responsible groups that made the treated OPF a better material for heavy metal sorption. Meanwhile, the nitrogen-containing groups as confirmed with FTIR results suggested the active role of these groups in binding the Na^+ ions through the formation of dative covalent bond after the treatment to create suitable exchange sites for heavy metal removal [1].

Thermogravimetry

Thermogravimetry analysis was also used to characterize the OPF before and after the treatment process with NaOH. From the TGA curves (Fig. 4), the differences between untreated and NaOH treated OPF can be noted. The first stage of weight

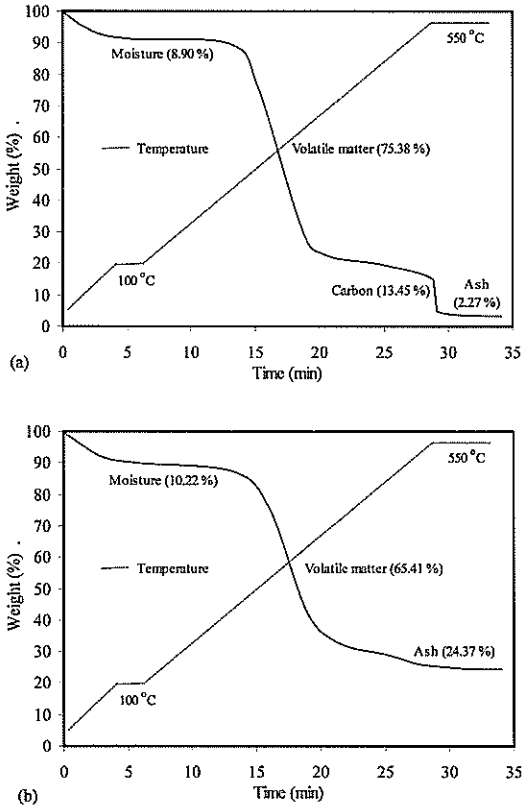

Figure 4. TGA result of OPF. (a) before NaOH treatment, and (b) after NaOH treatment.

loss began at about 100°C for both materials with weight loss of about 9-10 % due to loss of physically sorbed water from the biomass surfaces [16]. The second stage weight loss occurred at 240-410°C for the untreated OPF and slightly lower, i.e. 230-390°C for NaOH treated biomass. The magnitude of weight loss at this stage for the untreated biomass was 75.4 % while it was only 65.4 % for the treated biomass. This weight loss was attributed to the pyrolysis of the biomass to form volatile hydrocarbons. For the untreated OPF, about 13.5 % of combustible carboneceous content was detected when the TGA gas was shifted from nitrogen to oxygen at 550°C for 10 min. However, this fraction was not clearly observed with the NaOH treated OPF. The TGA results also suggested that the untreated OPF contained 2.3 % of ash (inorganic content) while it was significantly higher at 24.4 % in NaOH treated OPF.

After the NaOH treatment, a reduction in the amount of volatile matter was observed. This result agreed with the FTIR result that detected the disappearance of methyl groups, primarily belonging to pectin component of OPF. Besides, the solubilization of hemicellulose in the base solution also led to the extraction of this pentose-rich fraction from the biomass. Consequently, the loss of those fractions manifested as the lower amount of volatile fraction of OPF in the treated biomass. The loss of volatile matter in NaOH treated biomass also started at relatively higher temperature (240°C compared to 230°C for NaOH treated OPF) as hemicellulose and pectin were substances of relatively lower H/C ratio that were theoretically more resistant to pyrolysis [15]. This result was consistent with that obtained through thermogravimetric analysis. The ash content, which indicated the amount of inorganic substances, increased after the treatment process. This increase was due to the higher amount of Na^+ ions that was retained in the biomass after the treatment with NaOH. It was expected that a rather strong electrostatic interaction could be involved and responsible for the retention of Na ions in the biomass. This result led to the conclusion that Na ions acted as the counter ion to the nitrogen- and sulphur-containing functional groups in the NaOH treated biomass. The presence of these two types of functional groups was detected and confirmed through FTIR and elemental analyses.

CONCLUSION

NaOH treatment of OPF significantly improved heavy metal sorption capacity of the biomass while reducing the sorption time. Observed changes in the surface morphology, coupled with the result of elemental composition analysis, suggested the solubilization of hemicellulose and pectin from OPF. It was detected as visible shrinkage in the material and reduced number of terminal $-CH_3$. TGA results gave strong indication that Na^+ was the counter ion in the treated biomass for exchange with heavy metals during the sorption process. The higher nitrogen-containing groups in NaOH-treated OPF as confirmed by elemental analysis acted as the negatively charged functional groups through dative covalent bond formation that bound Na to be subsequently exchanged with heavy metal during the sorption process. The sulfur-containing functional groups could also play the same role, but of less importance.

Journal of Science and Technology in the Tropics (2007) 3: 5-9

Quality assurance: Towards diagnostic parasitology practices par excellence

Praphathip Eamsobhana
Department of Parasitology, Faculty of Medicine Siriraj Hospital,
Mahidol University, Bangkok 10700, Thailand
(Email: sipes@mucc.mahidol.ac.th)

Abstract Quality assurance in the diagnostic parasitology laboratory is essential for providing reliable, precise and accurate results of parasite investigations in support of optimal patient care, epidemiological surveillance and research. Many factors may influence the quality in a parasitology laboratory – pre- and post-analytical elements as well as analytical procedures. Quality assurance requires, among others, internal quality control (IQC), external quality assessment (EQA), good laboratory practice (GLP), and continuous quality improvement (CQI). The rewards of a good Quality Assurance programme include: (1) generation of a quality/reliable service to benefit the laboratory user; (2) helping the physician in establishing proper diagnosis rapidly, thus generating confidence in him/her and better health care for the patient; (3) creation of good reputation for the laboratory; (4) motivation factor for the staff to perform better; (5) mandatory requirement for accreditation – e.g. ISO 15189; and (6) prevention of legal suits and associated complications.

Keywords quality assurance – diagnostic parasitology – good laboratory practice –quality control – quality assessment

INTRODUCTION

Quality Assurance (QA) in the laboratory setting is the total process whereby the quality of laboratory reports can be guaranteed. In the medical context, it means "The right result at the right time on the right specimen from the right patient, with result interpretation based on correct reference data, and at the right price". Quality assurance is of paramount importance as unreliable results could have serious consequences for the health of the individual or community. Its main objective is to provide reliable laboratory data in health care activities and to ensure comparability of results [1, 2].

In the diagnostic parasitology laboratory, quality assurance is essential for providing reliable, precise and accurate results of parasite investigations in support of optimal patient care, epidemiological surveillance and research. The medical parasitology laboratory is responsible for providing accurate information on detection and identification of parasites for clinical diagnosis of patients and in support of public health activity.

FACTORS INFLUENCING QUALITY IN PARASITOLOGY LABORATORY

Many factors may influence the quality in a parasitology laboratory. The reliability of laboratory results depends on pre- and post-analytical elements as well as analytical procedures [3-5]. In addition, para-analytical factors may be sources of error that are beyond the control of the laboratory staff.

Analytical quality control

The determinants that govern analytical quality control include:

- Selection of right technique of proven efficacy
- Procedural reliability using standard operating procedures manual
- Equipment reliability

REFERENCES

1. Shukla S.R. and Pai R.S. (2005) Adsorption of Cu (II), Ni (II) and Zn (II) on modified jute fibres. *Bioresource Technology* **96:** 1430-1438.
2. Jeon C. and Höll W.H. (2003) Chemical modification of chitosan and equilibrium study for mecury ion removal. *Water Research* **37:** 4770-4780.
3. Ngah W.S.W., Ghani S.A. and Kamari A. (2005) Adsorption behavior of Fe (II) and Fe (III) ions in aqueous solution on chitosan and cross-linked chitosan beads. *Bioresource Technology* **96:** 443-450.
4. Yacob S., Hassan M.A., Shirai Y., Wakisaka M. and Subash S. (2006) Baseline study of methane emission from anaerobic ponds of palm oil mill effluent treatment. *Science of the Total Environment* **366:** 187-196.
5. Chubar N., Carvalho J.R. and Correia M.J.N. (2004) Heavy metal biosorption on cork biomass: Effect of the pre-treatment. *Colloids and Surfaces* **238:** 51-58.
6. Shukla S.R. and Pai R. S. (2005) Removal of Pb(II) from Solution Using Cellulose-Containing Materials. *Journal of Chemical Technology and Biotechnology* **80:** 176-183.
7. Kapoor A. and Viraraghavan T. (1998) Biosorption of heavy metals on *Aspergillus niger*: Effect of pretreatment. *Bioresource Technology* **63:** 109-113.
8. Sauthichak B., Nakano K., Nomura M., Chiba N. and Nishimura O. (2006) Phragmites australis: A novel biosorbent for the removal of heavy metals in aqueous solution. *Water Research* **40:** 2295-2302.
9. Salamatinia B., Kamarudin A.H., Abdullah A.Z. (2006) Optimization of Cu and Zn removal using pre-treated oil palm frond (OPF) by response surface methodology. *Iranian Journal of Chemical Engineers (IJChE)* **3**(2): 73-83.
10. Ajmal M., Rao R.A.K., Ahmad R. and Ahmad J. (2000) Adsorption studies on citrus reticulate (fruit peel of orange): Removal and recovery of Ni(II) from electroplating wastewater. *Journal of Hazardous Materials* **B79:** 117-131.
11. Basci N., Kocadagistan E. and Kocadagistan B (2004) Biosorption of copper (II) from aqueous solutions by wheat shell. *Desalination* **164:** 135-140.
12. Nagase H., Inthorn D., Isaji Y., Oda A., Kazumasa H. and Miyamoto K. (1997) Selective cadmium removal from hard water using NaOH-treated cells of the cyanobacterium *Tolypothrix tenuis*. *Journal of Fermentation and Bioengineering* **84:** 151-157.
13. Altundogan H.S. (2005) Cr (VI) Removal from aqueous solution by iron (III) hydroxide-loaded sugar beet pulp. *Process Biochemistry* **40:** 1443-1452.
14. Villaescusa I., Fiol N., Martinez M., Miralles N., Poch J. and Serarols J. (2004) Removal of copper and nickel ions from aqueous solutions by grape stalks wastes. *Water Research* **38:** 992-1002.
15. Kapoor A. and Viraraghavan T. (1997) Heavy metal biosorption sites in *Aspergillus niger*. *Bioresource Technology* **61:** 221-227.
16. Sankararamakrishnan N. and Sanghi R. (2006) Preparation and characterization of a novel xanthated chitosan. *Carbohydrate Polymers* **45:** 123-132.

Journal of Science and Technology in the Tropics (2006) **3:** 51-57

Development of seismic hazard maps for Peninsular Malaysia

Azlan Adnan, Hendriyawan, Aminaton Marto, Masyhur Irsyam
Structural Earthquake Engineering Research, Structure and Materials Laboratory D04-242
Faculty of Civil Engineering-Universiti Teknologi Malaysia
81310 UTM Skudai, Johor Bahru, Malaysia
(Email: azlan@seer.org.my)

Received 06.11.2006; accepted 18.01.2007

Abstract This paper presents the development of seismic hazard maps for Peninsular Malaysia using total probability theorem. The analysis covers the development of seismotectonic model, the determination of seismic hazard parameters, and the selection of appropriate attenuation relationships for Peninsular Malaysia. Logic tree method was performed in the analysis in order to take into account the epistemic uncertainties by including alternative interpretations, models, and parameters that were weighted in the analysis according to their probability of being correct. Two macrozonation maps representing 10% and 2% probability of exceedance (PE) in 50 years ground motions for Peninsular Malaysia were developed in this study. The results show the ground motions across the Peninsular Malaysian range between 2% g (20 gal) and 10% g (100 gal) for 10% PE in 50-year hazard levels and between 4% g (40 gal) and 20% g (200 gal) for 2% PE in 50-year hazard levels. The hazard levels show the peak ground acceleration contours increase from the northeast to the southwest of Peninsular Malaysia.

Keywords seismic hazard assessment – total probability theorem – macrozonation study

INTRODUCTION

Earthquake is one of the most devastating natural disasters on the earth. Earthquakes can affect hundreds of thousands of square kilometers; causing damage to structures or infrastructures facilities; result in loss of life and injury to hundreds of thousands of persons; and disrupting the social and economic functioning of the affected area. Usually the effects will rise significantly as a result of increases in population and structures or infrastructures facilities. Although it is impossible to prevent earthquake from occurring, it is possible to mitigate the effects of strong earthquake shaking and to reduce the loss of life, injuries and damages. The most effective way to reduce disasters caused by earthquakes is to estimate the seismic hazard and to apply it in the design of buildings and other structures. Thus, research in earthquake engineering is useful to mitigate the large earthquakes that may occur in the future.

This paper presents the macrozonation study for developing PGA contour map for Peninsular Malaysia. The paper describes the earthquake data processing techniques, the development of new seismotectonic model, the determination of seismic hazard parameters, and the selection of appropriate attenuation relationships for Peninsular Malaysia. The macrozonation maps were developed using Probabilistic Seismic Hazard Assessment (PSHA). The epistemic uncertainties due to lack of data and instrumental measurements were solved in this research by using logic tree method.

EARTHQUAKE DATA

Seismic hazard assessment requires as complete a history as possible of earthquakes in or near the region of interest. The earthquake catalogue used in this study was based on compilation of several catalogues from local and international institutions, such as International Seismological Center (ISC), National U.S. Geological Survey (USGS), Malaysian Meteorological Department (MMD) and

other catalogs.

The combined catalogue covers an area from 90°E to 125°E longitude and 10°S to 10°N latitude. From the catalog dating from 13 May 1897 to 31 December 2004, there are a total of 14119 earthquake events. The minimum magnitude is 5.0 and the maximum depth is 200 km.

Typical characteristics of earthquake catalogues are as follows: (1) the magnitude scales used in the catalogs are not uniform, due to the fact that the earthquake events were recorded using more than one type of instrument; (2) the earthquake catalogs contain both the main shock events and the accessory shock events (foreshock and aftershock events), hence the data are not valid to be used when the temporal occurrence of earthquakes are analyzed using Poisson model; and (3) the small events are usually incomplete in earthquake catalogs due to the limited sensitivity and coverage of the earth by seismographic networks.

The first problem is solved by choosing a consistent magnitude for seismic hazard assessment (SHA), and then the other magnitude scales are converted to the chosen magnitude scale by using empirical correlation [1-3]. In this research, a moment magnitude, Mw, is chosen as a measurement to quantify the size of earthquake. Other types of magnitude in the catalogs were then converted to Mw by using empirical correlations. The map showing the locations of the earthquake epicentres for the period of observation (1897-2004) was then developed (Fig. 1).

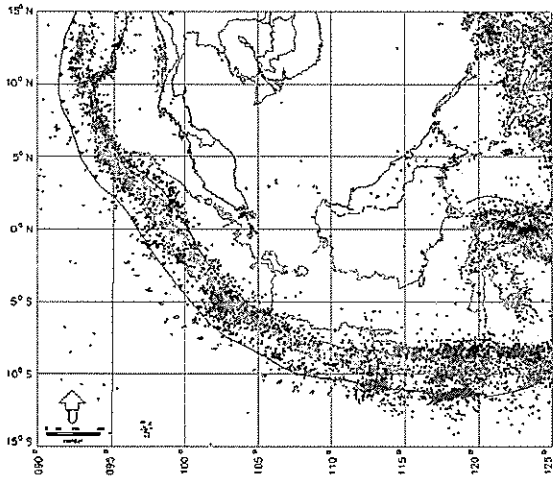

Figure 1. Historical earthquakes (Mw > 5.0) around Malaysia from 1897-2004.

The second problem is solved by declustering the catalog using time and distance windows criteria [4]. The criteria proposed by Gardner and Knopoff [4] were used in this research because this criteria have considered the time and distance windows for magnitude above 8.0. The algorithm eliminates 9059 accessory shock events. The combined catalog, after removal of accessory shock events, contains 5060 records or more than 50% of earthquake records have been eliminated in the combined catalog. Out of 5060 records, 967 records are from the Sumatra faults.

The third problem is solved by performing catalog completeness analysis. In this study, historical earthquake data between 1900 and 2004 were analyzed for completeness using Stepp method [5]. Based on the catalog completeness analysis of the general Southeast Asia regions (Fig. 1), the earthquakes within interval $5.0 \leq M_w < 6.0$ are completely reported only during the most recent 28 year interval or since 1978, interval $6.0 \leq M_w < 7.0$ are completely reported during the most recent 33 year interval or since 1972, and magnitude more than 7.0 are completely reported over 104-year sample interval.

TECTONIC SETTING

Based on the location of Peninsular Malaysia, the general tectonic features can be divided into two seismic source zones (Fig. 2). The first seismic source zone is the Sumatra subduction zone (SSZ). All earthquakes that occurred near the convergent boundaries where Indo-Australian plate is being subducted under Eurasian plate are classified into this zone. The Indo-Australian plate is sliding approximately northward beneath Sumatra and Java, where the direction of convergence is N20°E and the overall rate of convergence is 7.7-cm/year [6].

The second seismic source zone is called the Sumatra fault zone (SFZ). All earthquakes that occurred due to strike slip movement along clearly defined fault in the frontal arc area of Sumatra Fault are classified into this zone. The Sumatra fault is about 1900 km long structure that accommodates right lateral strike slip associated with the oblique convergence along the plate margin. Several large earthquakes have occurred in this zone. Some earthquake events that occurred in this zone were

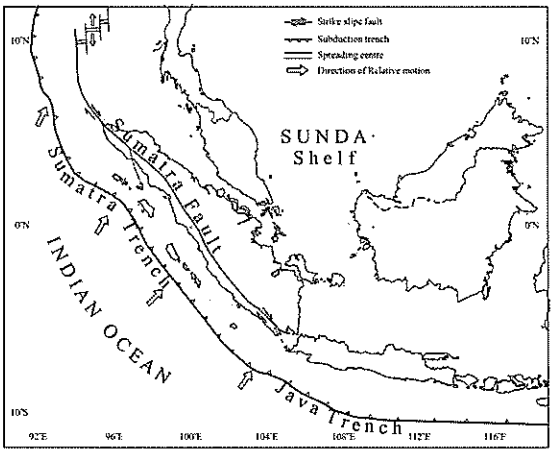

Figure 2. Tectonic setting around Peninsular Malaysia [7].

the 1926 Padang Panjang (M_S = 6.75), the 1933 Liwa (M_S=7.5), the 1964 Aceh (m_b = 6.7) and the 1993 Liwa (M_S = 7.2) earthquakes.

SEISMIC HAZARD ASSESSMENT

In this research, seismic hazard assessment for Peninsular Malaysia is performed using total probability theorem (PSHA) [8,9], which assumed the earthquake magnitude, M and the hypocenter distance, R as a continuous independent random variable. The expected ground acceleration for a particular site with specified mean return period is defined by a seismic hazard analysis procedure.

The total probability theorem can be represented in the most basic form as follows:

$$P[I \geq i] = \int_r \int_m P[I \geq i | m \text{ and } r].f_M(m).f_R(r)\, dm\, dr \quad (1)$$

where, f_M is the density function of magnitude, f_R is the density function of hypocenter distance, and P [I > i |M and R] is the conditional probability of (random) intensity I exceeding value I, at the site for a given earthquake magnitude, M and hypocenter distance, R.

Generally, the method could be divided into four stages [10] as follows: (i) identification and characterization of all earthquake sources including the probability distribution of potential rupture locations within the source, (ii) characterization of seismicity or temporal distribution of earthquake, (iii) determination of ground motion produced at the site by earthquakes at any possible point in each source zone, and (iv) prediction of ground motion parameters that will exceed during a particular time period.

Identification and characterization of seismic sources

A seismic source zone is defined as a seismically homogenous area, in which every point within the source zone is assumed to have the same probability of being the epicenter of a future earthquake [11]. In this research, the seismic source was investigated by plotting the spatial distribution of earthquakes using the regional seismicity data recorded since 1897 and then combining with the seismotectonic setting to develop seismic sources for Peninsular Malaysia. In order to simplify the analysis, both seismic source zones are segmented into seven sub zones (Fig. 3). Cross sections of every seismic zone can be seen in Figure 4. Based on the dip angles and the focal depth of focus, subduction zones were divided into Megathrust zone and Benioff zone (Fig. 4).

Characterization of seismicity

Characterization of seismicity at a particular site or region is commonly expressed in seismic hazard parameters. Seismic hazard parameters are needed for fully describing earthquake activity within the earth crust in a certain region. There are three parameters that are most commonly considered in seismic hazard assessment, i.e. a-b parameter,

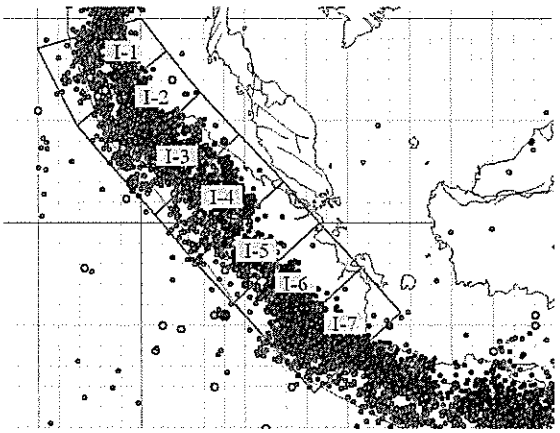

Figure 3. Seismic Source zones around Peninsular Malaysia.

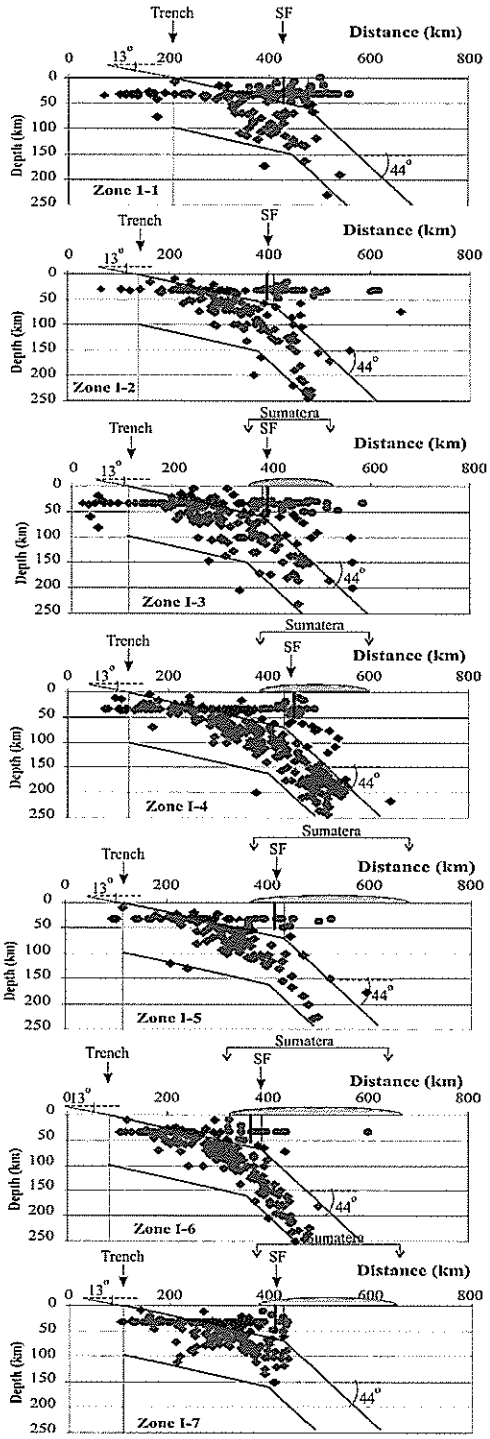

Figure 4. Hypocentre profiles.

recurrence rate, and maximum size of future earthquakes for each source. Usually, temporal distribution of earthquakes is assumed to follow frequency-magnitude relationship proposed by Gutenberg-Richter (G-R) [12].

The simplest method to obtain a-b value is the least square method (LS). The disadvantage of LS method is that it cannot be used directly to calculate the mean annual rate of exceedance from combining different completeness catalogues. Usually, this method produces overestimated b values that cause the rates of large earthquakes to be underestimated. Several researchers [13-16] have proposed alternative methods to obtain a-b values and to minimize bias. These methods have accounted the relationship between earthquake data and interval time when the catalogues are homogeneous. The seismicity parameters for each source zone used in this analysis can be seen in the recurrence relationship chart (Fig. 5).

Attenuation relationship

One of the critical factors in seismic analysis is to obtain or to select appropriate attenuation relationship. This formula, also known as ground motion relation, is a simple mathematical model that relates a ground motion parameter (i.e. spectral acceleration, velocity and displacement) to earthquake source parameter (i.e. magnitude, source to site distance, mechanism) and local site condition [17].

A number of attenuation relations has been derived in the last two decades as the instrumental record of ground motions have become more available. In general, they are categorized according to tectonic environment (i.e. subduction zone and shallow crustal earthquakes) and site condition. There are several attenuation relationships derived for subduction zone earthquake, which are commonly used, such as Youngs *et al.* [18] and Petersen *et al.* [19], whereas attenuation relationships, which were developed by Campbell [17] and Sadigh *et al.* [20] are frequently used to estimate ground motion for shallow crustal earthquake. In this research attenuation proposed by Azlan *et al.* [21] and Petersen *et al.* [19] were used to predict ground motion due to SSZ while attenuation proposed by Campbell [17] was used for SFZ. These attenuations were chosen because they were derived for earthquake distance of up to 1000 km.

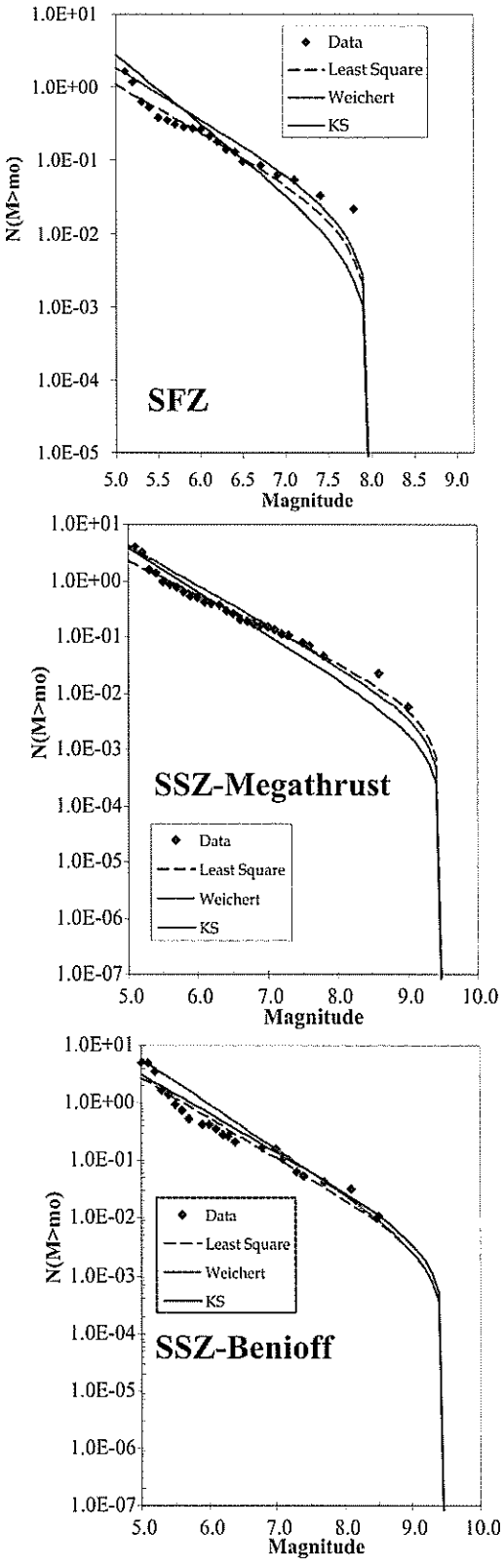

Figure 5. Recurrence relationship models for Peninsular Malaysia.

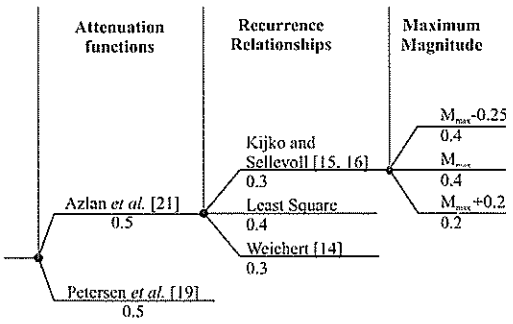

Figure 6. Logic tree model for incorporation of model uncertainty.

Logic tree

Epistemic uncertainty is included in the PSHA by explicitly including alternative hypotheses and models. The logic tree allows a formal characterization of uncertainty in the analysis by including alternative interpretations, models, and parameters that are weighted in the analysis according to their probability of being correct. Logic trees [22, 23] are used in this study in order to allow uncertainty in selection of models for attenuation, recurrence rate, and maximum magnitude to be considered. In this research, attenuation proposed by Azlan *et al.* [21] and Petersen *et al.* [19] were assigned, a relative likelihood of 0.50 each. The recurrence rates calculated according to the method of Weichert [14] and that of Kijko and Sellevoll [15, 16] were considered equally likely to be correct whilst the least square method was assigned a relative likelihood of 0.4. At the final level, different relative likelihoods were assigned to the maximum magnitude. The logic tree model is shown in Figure 6.

RESULTS OF ANALYSIS AND CONCLUSIONS

The contour maps of PGA at 10% and 2% probabilities of exceedance in 50 years for bedrock of Peninsular Malaysia can be seen in Figure 7. The PGA across Peninsular Malaysia have a range of between 20 and 100 gals for 10% probability of exceedance (PE) in 50 years hazard levels or 500-year return period of earthquake and between 40 and 200 gals for 2% in 50-year hazard levels or 2500-year return period of earthquake. The hazard levels

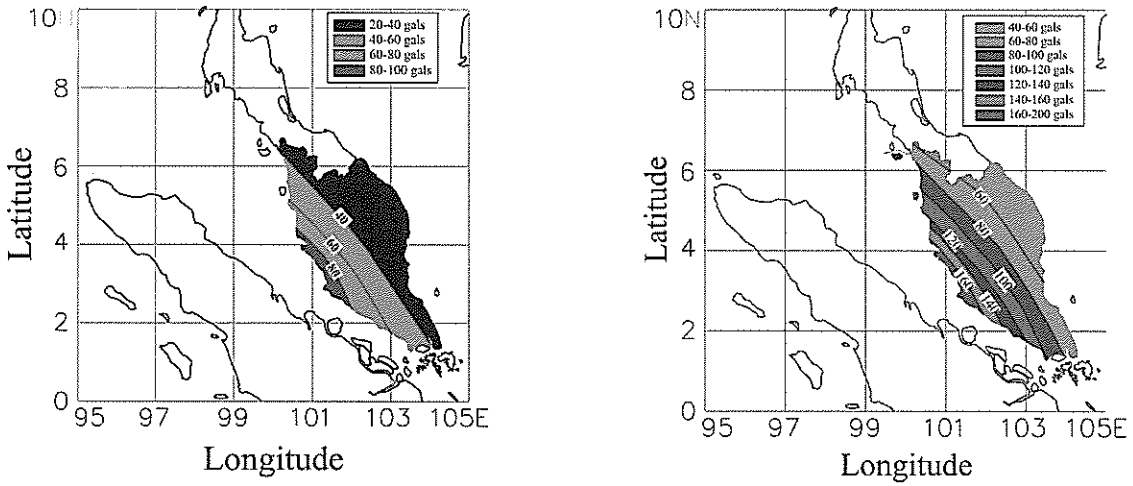

(a) PGA map for 10% PE in 50 years (500 years return period).

(b) PGA map for 2% PE in 50 years (2500 years return period).

Figure 7. Seismic hazard maps of Peninsular Malaysia.

show the PGA contours increase from the northeast to the southwest of Peninsular Malaysia.

Acknowledgment – The procedure described in this paper has been developed as part of a project funded by the Construction Industry Development Board (CIDB) Malaysia, entitled "Seismic Hazard Analysis of Peninsular Malaysia for Structural Design Purposes". This support is gratefully acknowledged.

REFERENCES

1. Geller R.J. (1976) Scaling Relations for Earthquake Source Parameters and Magnitudes. *Bulletin of the Seismological Society of America* **66:** 1501-1523.
2. Rong Y. (2002) *Evaluation of Earthquake Potential in China.* University of California Los Angeles: PhD Thesis.
3. EPRI (1994) *The Earthquake of Stable Continental Regions, Vol. I: Assessment of Large Earthquake Potential.* File Report Electric Power Research Institute, Palo Alto, California.
4. Gardner J.K. and Knopoff L. (1974) Is the Sequence of Earthquakes in Southern California, with Aftershocks Removed, Poissonian? *Bulletin of the Seismological Society of America* **64:** 1363-1367.
5. Stepp J.C (1973) *Analysis of the Completeness of the Earthquake Hazard Sample in the Puget Sound Area.* NOAA Technical Report, ERL 267-ESL 30. Boulder, CO: pp. 16-28.
6. DeMets C., Gordon R.G., Argus D.F. and Steia S. (1990). Current Plate Motions. *Geophysics Journal International* **101:** 425-478.
7. Huchon P. and Le Pichon X. (1984) Sunda Strait and Central Sumatra Fault. *Journal of Geology* **12:** 668-672.
8. Cornell C.A. (1968) Engineering Seismic Risk Analysis. *Bulletin of the Seismological Society of America* **58:** 1583-1606.
9. Merz H.A. and Cornell C.A (1973) *Aftershocks in Engineering Seismic Risk Analysis.* Report R73-25. Massachusetts: Department of Civil Engineering, MIT, Cambridge.
10. Reiter L. (1990) *Earthquake Hazard Analysis-Issues and Insights.* New York. Columbia University Press.
11. Erdik M., Doyuran V., Yucemen S., Gulkan P. and Akkas N. (1982) A Probabilistic Assessment of the Seismic Hazard in Turkey for Long Return Periods. *Proc. 3rd International Earthquake Microzonation Conference.* Seattle, Washington.
12. Guttenberg B. and Richter C.F. (1954) *Seismicity of the Earth.* Princeton, New Jersey: Princeton University Press.
13. Dong W.M., Bao A.B. and Shah H.C. (1984) Use of Maximum Entropy Principle in Earthquake Recurrence Relationships. *Bulletin of the Seismological Society of America* **74:** 725-737.
14. Weichert D.H. (1980) Estimation of the Earthquake Recurrence Parameters for Unequal Observation Periods for Different Magnitudes. *Bulletin of the Seismological Society of America* **70:** 1337-1346.
15. Kijko A. and Sellevol M.A. (1989) Estimation of

Earthquake Hazard Parameters from Incomplete Data Files Part I. Utilization of Extreme and Complete Catalog with Different Threshold Magnitudes. *Bulletin of the Seismological Society of America* **79:** 645-654.

16. Kijko A. and Sellevol M.A. (1992) Estimation of Earthquake Hazard Parameters from Incomplete Data Files Part II. Incorporation of Magnitude heterogeneity. *Bulletin of the Seismological Society of America* **82:** 120-134.
17. Campbell K.W. (2003) Prediction of strong ground motion using the hybrid empirical method and its use in the development of ground-motion (attenuation) relations in Eastern North America. *Bulletin of the Seismological Society of America* **93:** 1012–1033.
18. Youngs R.R., Chiou S.J., Silva W.J. and Humphrey J.R. (1997) Strong Ground Motion Attenuation Relationships for Subduction Zone Earthquake. *Seismological Research Letters* **68:** 58-74.
19. Petersen M.D., Dewey J., Hartzell S., Mueller C., Harmsen S., Frankel A.D. and Rukstakels (2004) Probabilistic Seismic Hazard Analysis for Sumatra, Indonesia and Across the Malaysian Peninsula. *Tectonophysics* **390:** 141-158.
20. Sadigh K., Chang C.Y., Egan J.A., Makdisi F. and Youngs R.R. (1997) Strong Ground Motion Attenuation Relations for Shallow Crustal Earthquakes Based on Californian Strong Motion Data. *Seismological Research Letters* **68:** 190-198.
21. Azlan Adnan, Hendriyawan, Aminaton Marto and Masyhur Irsyam (2005) Selection and Development of Appropriate Attenuation Relationship for Peninsular Malaysia. *Proceeding Malaysian Science and Technology Congress 2005.* Mid Valley, Kuala Lumpur.
22 Kulkarni R.B., Youngs R.R. and Coppersmith K.J. (1984) Assessment of Confidence Interval for Results of Seismic Hazard Analysis. *Proceeding 8th World Conference on Earthquake Engineering.* San Francisco 1: 263-270.
23. Coppersmith K.J. and Youngs R.R. (1986) Capturing Uncertainty in Probabilistic Seismic Hazard Assessment with Intraplate Tectonic Environment. *Proceedings 3rd U.S. National Conference on Earthquake Engineering.* Charleston, South Carolina 1: 301-312.

Journal of Science and Technology in the Tropics (2007) **3**: 59

Goats: Biology, Production and Development in Asia

by C. Devendra (2007) Kuala Lumpur: Academy of Sciences Malaysia
Hardcover, 246 + xxi pp, RM 180

This book discusses the biology, production and development of goats in Asia. It summarizes available information on the contribution and potential of goats to enhance animal protein supplies.

The book describes the biological peculiarities and features in goats, adaptation, geographical distribution, diversity of breeds, role in farming systems, multiple contributions, and their value in meat, milk, fibre and skin production. It discusses increased productivity through more efficient use of available indigenous breeds, improved production in production-to-consumption systems, issues concerning the links to food security, alleviation of poverty and improved livelihoods of the poorest of the poor, and development strategies. It is organized in organized in 12 chapters – evolution and domestication, goats in farming systems, agro-ecological zones and the environment, breeds, bioclimatology and adaptation, goat production systems, meat and milk production, feed resources and nutrition to improve productivity, improved husbandry and economic potential, post-production systems, development strategies, and research for development – and illustrated with 62 colour photographs.

Apart from typographical errors, some fundamental aspects of biology were not dealt with. For example, as a student of biology one would like to know about the karyotype (chromosome constitution) and gene diversity as well as genetic variation among the various breeds. It would also have been useful to have a chapter on pests, parasites and diseases and their impacts on production.

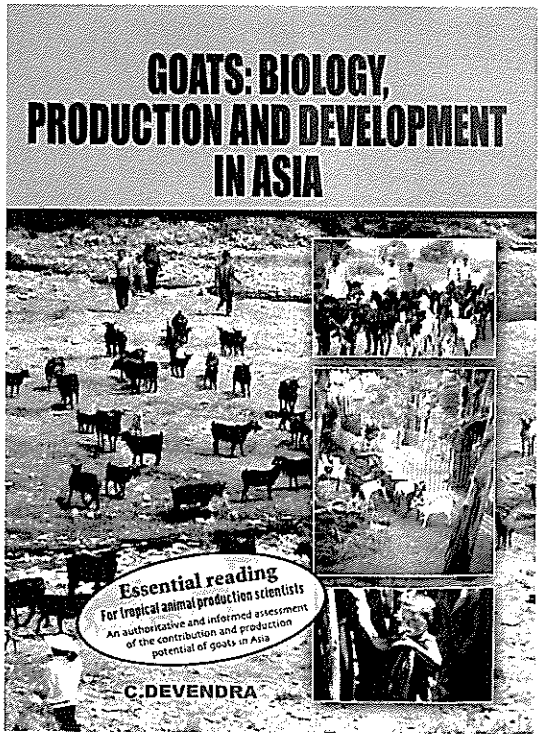

The publication is available from:
Academy of Sciences Malaysia
(attn: Mohd Zairi Mansor)
902-4 Jalan Tun Ismail
50480 Kuala Lumpur
Malaysia
Tel: 03-2694 9898
Fax: 03-2694 5858

- Reagent stability, integrity and efficiency
- Proficiency of personnel and continuous updating of knowledge
- Good internal quality control
- Participation in external quality assessment programmes

Para-analytical quality control

Para-analytical quality control can be divided into pre-analytical and post-analytical components. The pre-analytical components include: right investigation; right sample; right collection; right laboratory; right transportation; right labeling; and right quantity. The post-analytical components comprise: accurate recording; correct interpretation; reasonable turnaround time; available guidance; disposal of sample; and waste management.

QUALITY ASSURANCE IN DIAGNOSTIC PARASITOLOGY

Quality assurance (QA) is the mutual responsibility between laboratory personnel and clinicians [5]. There should therefore be frequent dialogues between the laboratory persons and the physicians for appropriate use of the facilities and right interpretation of the results obtained in the laboratory.

Quality assurance cannot be achieved through improving and controlling the analytical process without parallel improvement and control of pre-analytical and post-analytical procedures. It requires, among others, internal quality control (IQC), external quality assessment (EQA), good laboratory practice (GLP), and continuous quality improvement (CQI) [1, 2, 5].

Internal quality control

Internal quality control (IQC) is the set of procedures undertaken by the laboratory staff for the continuous and immediate monitoring of laboratory work, in order to decide whether the results are reliable enough to be released. Its main objective is to ensure day-to-day consistency (precision) in the test parameters. The procedures have an immediate effect on the laboratory performance as they actually check every step in the analytical process [1, 2, 5].

Quality control in clinical parasitology must cover all aspects from the decision to collect the specimen to the interpretation of report. Any break in the chain would ultimately lead to generation of a faulty report. Accuracy of report can be guaranteed only when appropriate quality control measures form an integral part of SOP (standard operating procedures) in the laboratory.

Quality control programmes in diagnostic parasitology ensure the accurate, reliable and reproducible report generated by the laboratory. It is achieved by (a) assessing the quality of specimens; (b) monitoring the performance of test procedures, reagents, media, equipment and personnel; and (c) reviewing test results and documenting the validity of the test method.

Guidelines for quality control parameters

The quality control parameters in parasitology laboratory include the following:

1. Specimen collection
   - provide instructions for collection and transportation
   - establish criteria for acceptable specimens
   - establish rejection criteria for unacceptable specimens
2. Procedural manual
   - define test performance, specimen acceptability
   - reagent preparation, QC calculations and reporting
   - review annually
   - available at work area
3. Personnel
   - use sufficient qualified personnel depending on complexity of work
   - provide continuing technical education
   - provide with written performance standards
   - evaluate competency of laboratory personnel annually
4. QC records
   - record all QC results on prescribed forms
   - report all out-of-control observations to supervisor
   - note corrective action on QC forms
   - review QC records monthly
5. Patient reports
   - report only to authorized personnel
   - notify test requester of important (panic) result immediately
   - correct errors in patient's report in timely manner

Journal of Science and Technology in the Tropics (2007) **3**: 60

Tropical Horticulture and Gardening

by Francis S. P. Ng (2006) Kuala Lumpur: Academy of Sciences Malaysia
Hardcover, 361 + xii pp, RM 260

This is a book for avid amateurs and those with professional or semi-professional interests in tropical horticulture and gardening. Landscapers, managers of parks and gardens, property developers and students of horticulture will find here explanations of fundamental concepts and principles, a pictorial guide to 1000 types of ornamental plants in systematic order, and notes on their cultivation and propagation.

All plants covered in the book are traced to their historical origins, and those of special cultural and economic interest are highlighted. The major steps leading to our present understanding of plants, from classification and nutrition to behavioural patterns under tropical conditions are explained. In addition, major gardens in the world are reviewed to provide tropical practitioners with a better understanding of their art in a global and historical context.

The book is organized in 9 chapters – Plant Domestication: 8000 BC to AD 2000; The Knowledge System for Plants; Plant Form and Habit; Ferns and Fern Allies; Gymnosperms; Flowering Plants: Monocots; Flowering Plants: Dicots; Garden Design; Plants and the Tropical Environment – and illustrated with over 1300 colour photographs. Some ornamental plants, such as cacti, orchids and roses, are not included in this book.

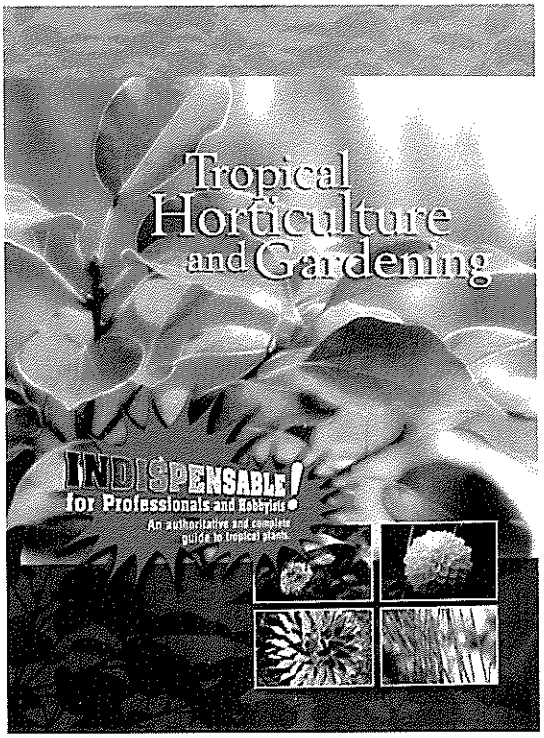

For information, contact:
Academy of Sciences Malaysia
(attn: Mohd Zairi Mansor)
902-4 Jalan Tun Ismail
50480 Kuala Lumpur
Malaysia
Tel: 03-2694 9898
Fax: 03-2694 5858

- retain records at least for two years

6. Referral specimens
   - use only authorized referral laboratory
   - include name of reference laboratory on patient's report
7. Proficiency testing
   - participate in appropriate external quality assessment scheme
   - consider internal proficiency-testing programme
8. Equipment performance
   - document function checks of equipment
   - perform as frequently as recommended by manufacturer
   - document routine preventive maintenance
   - retain maintenance records for life equipment
9. Stains and reagents
   - label containers as to contents; concentration; storage requirement; date prepared, received/ placed in service; shelf life
   - store as per recommendations
   - test with positive and negative controls prior to use
   - discard outdated material and reagents that fail to perform
10. User prepared media
    - record amount prepared, source, lot no., sterilization method, preparation date, pH, expiration date
    - test media with QC organisms of known characters
11. Commercial kits
    - test each batch as per recommendations of manufacturer

External quality assessment

Internal quality control and external quality assessment would ensure the reliability of the analytical procedures, their results and finally the quality of investigations in a laboratory.

Quality assessment (= proficiency testing) is a process by which the performance of participating laboratories may be monitored. The process allows individual participants to become aware of any problems in their laboratories and take corrective action [2, 6, 7]. The information on performance may also be useful to national authority in evaluating standards, and in recommending the need for allocation of resources.

External quality assessment (EQA) is a system in which the laboratory results are scrutinized objectively by an outside agency in order to get a general impression of the standard of laboratory practice. It helps to achieve inter-laboratory comparability (accuracy) [2, 6-9].

As external quality assessment is retrospective, a laboratory cannot be notified until much later about a discrepant finding, and thus alerted to a problem at the time it occurs. Its aim is not the achievement of day-to-day consistency, but to help establish good laboratory practice (GLP). It is not a system for controlling specific tests, but a range of tests undertaken in the laboratories.

External quality assessment scheme

The external quality assessment scheme may be national or international in scope, viz. National External Quality Assessment Scheme (NEQAS) and International External Quality Assessment Scheme (IEQAS).

Under the National External Quality Assessment Scheme, the country concerned controls the quality of the laboratory procedures of the diagnostic laboratories in both the government and private sectors. In some countries, participation in the national scheme is mandatory for licensing [6, 9]. It is therefore preferable that a central government institution, while taking part in the IEQAS, should coordinate the NEQAS in the country. In a small country, the central laboratory could manage the EQAS for the peripheral and intermediate level laboratories. In a medium-sized country, a three-tier system may be necessary – central, intermediate and peripheral. For a large country, a four-tier system may be introduced – central, regional, intermediate and peripheral [2]. In Thailand, the institution is the Bureau of Laboratory Quality Standards, Department of Medical Sciences, Ministry of Public Health.

The International External Quality Assessment Scheme (IEQAS) has been established by the World Health Organisation, with the following objectives: (1) to identify, in each country, a small number of laboratories with a high standard of proficiency which will serve as reference centres; (2) to encourage these reference centres to be the focus for developing NEQAS; (3) to coordinate all the national schemes; and (4) to provide harmonization of different laboratory results on worldwide level [1,

2, 6, 7].

The WHO IEQAS is coordinated by the Health Laboratory Technology Unit, WHO HQ. It has six sections – clinical chemistry (organized by WHO Collaborating Center in Birmingham); clinical microbiology (WHO CC in Leuven); hematology (WHO CC in London); parasitology (WHO CC in Paris); immunochemistry (WHO CC in Dusseldorf); and HIV serology (WHO CC in London and Melbourne) [1, 2, 6].

Quality assessment scheme

The objectives of a quality assessment scheme are: (1) to provide assurance to consumers, viz. doctors and patients, that the laboratory results are of good quality; (2) to assess the quality of laboratory performance on a national and/or international scale; (3) to identify common errors and recommend corrective measures; (4) to encourage the use of standardized procedures and good quality reagents; and (5) to encourage and continue the application of the measures for internal quality control. This quality assessment scheme comprises the following components: organizing laboratory; participants; specimens; pre-distribution testing of specimens; documentation; distribution of specimens; testing of specimens by participants; analysis of results; and feedback of results.

For successful implementation, the quality assessment scheme should have a national Advisory Committee for all laboratory disciplines as well as a national Advisory Committee for individual laboratory disciplines. The Advisory Committee for all laboratory disciplines should be represented by professional associations, university academics and bureaucrats. They should lay down policy guidelines for all disciplines and meet at least once a year to discuss past year's performance and to set up programme for the coming years. Likewise, the Advisory Committee for individual laboratory disciplines should be tasked to formulate policy guidelines and provide technical supervision, and meet at least once a year to technically review the past year's reports [1, 2, 10, 11].

Basic principles of quality assessment scheme

Quality assessment is only one component in an assurance programme. It cannot be used as a substitute for quality control. The laboratories organizing quality assessment must be adequately funded on a continuing basis.

The specimens for quality assessment should provide participants with an insight into their performance with routine specimens. Failure with quality assessment of specimens usually indicates the presence of a problem with quality control procedures.

Quality assessment schemes are much more efficient at detecting differences in performance between participants than differences between methods and technique. It is essential that the participants are confident in the quality of the specimens used for quality assessment. The organizing laboratory therefore needs to devote considerable time and effort in ensuring this quality. It is also important that the participants receive the results soon after the exercise while they are still interested and are able to investigate the reasons for any incorrect results.

Quality assessment scheme is educational and aims at self-evaluation and self-help. It is therefore useful to have an Advisory Panel to provide help, advice and counseling to the poor performers. It is of paramount importance that the participants trust the confidentiality of the scheme.

Good laboratory practice

Internal quality control and external quality assessment are concerned specifically with actual test procedures. However, other parts of the process also require control if the tests are to be reliable. This requires good laboratory practices to ensure the performance of all activities in the best possible way so that the results obtained are of the highest possible accuracy [1, 2].

Good laboratory practice (GLP) encompasses: (1) proper collection of samples; (2) appropriate identification of specimen with special label in hazardous specimen; (3) prompt transportation to laboratory at appropriate temperature; (4) collection, analysis in the laboratory following which storage under conditions which prevent deterioration of the sample; (5) accurate performance of analysis; (6) release of reports after proper scrutiny; (7) delivery of reports to the correct destination in the shortest possible time; and (8) cordial relationship with the users [1, 2].

Continuous quality improvement

In addition to internal quality control, external quality assessment and good laboratory practice, quality assurance should aim at continuous quality improvement, not only by monitoring each step in the analytical process, but also by preventing errors through continuing (lifelong) education of the technical staff, improving the structure and the procedures, and better communication with the physicians requesting the service [1, 2].

CONCLUSION

The rewards of a good quality assurance programme include: (1) generation of a quality/reliable service to benefit the user; (2) helping the physician in establishing proper diagnosis rapidly, thus generating confidence in him/her and better health care for the patient; (3) creation of good reputation for the laboratory; (4) motivation factor for the staff to perform better; (5) mandatory requirement for accreditation – e.g. ISO 15189 [12]; and (6) prevention of legal suits and associated complications.

REFERENCES

1. El-Nageh M., Heuck C., Appel W., Vandepitte J., Engbaek K. and Gibbs W.N. (1992) *Basics of Quality Assurance for Intermediate and Peripheral Laboratories.* WHO Regional Publications. Eastern Mediterranean Series 2. WHO EMRO, Alexandria.
2. World Health Organization, Regional Office for South East Asia. (1994) *Health Laboratory Services in Support of Primary Health Care in Developing Countries.* SEARO Series No 24. New Delhi, WHO Regional Publications.
3. Barr J.T. (1999) Clinical laboratory utilization. In: Davis B.G., Mass D. and Bishop M.L. (eds.) *Principles of clinical laboratory utilization and consultation* pp 3-16. Philadelphia: WB Saunders Co.
4. Narayanan S. (2000) The preanalytic phase. An important component of laboratory medicine. *Am. J. Clin. Pathol.* **113:** 429-452
5. Tetrault G.A. (2001) Clinical laboratory quality assurance. In: Henry J.B. (ed) *Clinical Diagnosis and Management by Laboratory Methods* 20th ed. 20th ed, pp 148-156. Philadelphia; WB Saunders Co.
6. Deom A., El Aouad R., Heuck C.C., Kumari S., Lewis S.M., Uldall A. and Wardle J. (1999) Requirements and guidance for external quality assessment schemes for health laboratories. WHO/DIL/LAB/99.2. World Health Organization, Geneva.
7. Sciacovelli L., Zardo L., Secchiero S. and Plebani M. (2004) Quality specifications in EQA schemes: from theory to practice. *Clin. Chim. Acta* **346:** 87-97.
8. Rippey J.H. and Williamson W.E. (1988) The overall role of a proficiency testing program. *Arch. Pathol. Lab. Med.* **112:**340-342.
9. Duckworth J.K. (1988) Proficiency testing. Its role in a voluntary clinical Laboratory Accreditation Program. *Arch. Pathol. Lab. Med.* **112:**346-348.
10. ILAC-G13 (2000) *Requirement for the competence of provider of proficiency testing schemes.* National Association of Examination Authorities (NATA), Australia.
11. ISO/IEC 17011 (1995) *General requirements for bodies providing assessment and accreditation of conformity assessment bodies.* International Organization for Standardization, Geneva.
12. ISO/TC212(2003)*International Standard ISO 15189: Medical Laboratories – Particular Requirements for Quality and Competence.* Switzerland.